A NOVEL DEVICE FOR THE ESTABLISHMENT OF AN ANIMAL MODEL MIMICKING SPINAL DEFORMITY SURGERY FOR NEUROLOGICAL DEFICIT RISK MITIGATION

by

BRADLEY B ELMER

Presented to the Faculty of the Graduate School of
The University of Texas at Arlington in Partial Fulfillment
of the Requirements
for the Degree of

MASTER OF SCIENCE IN BIOMEDICAL ENGINEERING

THE UNIVERSITY OF TEXAS AT ARLINGTON
December 2010

ACKNOWLEDGEMENTS

First, I would like to thank Dr. Mario Romero-Ortega for giving me the opportunity to learn and work under his mentorship. I appreciate the trust, guidance, and encouragement he has given me since first joining his lab and throughout the length of my project. Through his mentoring, he has helped me acquire and refine new skills and abilities that will enhance my career in the future.

I could not have done anything without my team members, Dr. Jennifer L Seifert and Jennifer E Bell, and I would like to thank them for their incredible contributions and help with this project. Also, I would like to thank my other lab mates Eduardo Martinez, Swarup Dash, Parisa Lotfi, Collins Watson, and An Nguyen for their friendship and input on my research work.

I would like to thank Dr. Khosrow Behbehani and Dr. Young-tae Kim for serving on my thesis committee and for sharing their knowledge with me throughout my graduate career.

Most importantly, I would like to thank my wife Ashley and son Evan for their constant support, love, and confidence. And my father, Jerry B Elmer, and mother, Tanya L Elmer, for encouraging me to be the best I can be and instilling within me the desire to continually strive to educate myself.

November 22, 2010

ABSTRACT

A NOVEL DEVICE FOR THE ESTABLISHMENT OF AN ANIMAL
MODEL MIMICKING SPINAL DEFORMITY SURGERY
FOR NEUROLOGICAL DEFICIT
RISK MITIGATION

Bradley B Elmer, M.S.

The University of Texas at Arlington, 2010

Supervising Professor: Mario Romero-Ortega

Correction forces during spine deformity surgery impart significant multidirectional stress forces to the spinal cord, which in some cases result in severe damage to the spinal cord and permanent paralysis, the most feared complication. Animal models are critical for the development of neuroprotective strategies. However, those currently available are limited to contusion, transection, or unidirectional distraction injuries, which fail to replicate the multidirectional forces that occur during spine corrective surgery. In order to develop an improved model of distraction spinal cord injury we designed a device based on intervertebral grip fixation and linear actuators, capable of inducing controllable bidirectional distraction injury to the spine. The device was tested using a 7mm distention paradigm of the rat T10-12 vertebra. Behavior was assessed every twenty-four hours for seven days after injury, and all animals showed a drastic drop in the Basso, Beattie and Bresnahan (BBB) locomotor scale, from a normal 21 level to that of complete hind limb paralysis (0.17 +/- 0.41). The severity of this injury was confirmed by gross evaluation and histology using glial fibrillary acidic protein

immunocytochemistry for visualization of reactive gliosis. The high precision, control, and reproducibility of this bidirectional spine distraction device would contribute to the testing of neuroprotective strategies aimed at preventing unintended new neurological damage during corrective spine surgery.

TABLE OF CONTENTS

ACKNOWLEDGEMENTS iii

ABSTRACT iv

LIST OF ILLUSTRATIONS viii

LIST OF TABLES x

Chapter Page

1. INTRODUCTION 1

1.1 Incidence and Prevalence 1

1.2 Classification of SCI 1

1.2.1 Primary Mechanisms 1

1.2.2 Secondary Mechanisms 3

1.2.3 Current SCI and Neuronal Repair Treatment 4

1.3 Scoliosis 4

1.3.1 Intraoperative Prevention Against Neurological Deficit 6

1.4 Animal Models 7

1.4.1 Simple Models 7

1.4.2 Complex Models 8

1.5 Project Aims 9

2. DESIGN AND FABRICATION OF UTA DISTRACTOR DEVICE 10

2.1 Design Requirements 10

2.2 Design Details 11

2.2.1 Structural Components 11

2.2.2 Actuators 13

2.2.3 Supports and Guides 14

2.2.4 Load Cell 15
2.2.5 Custom Clamps 15
2.3 Bench Top Testing 17
2.4 Future Device Modifications 19
3. EXPERIMENTAL DISTRACTION INJURY 21
3.1 Methods 21
3.1.1 Device Preparation 21
3.1.2 Animal Procedure 21
3.1.3 Behavioral Analysis 22
3.1.4 Histology 23
3.2 Results and Discussion 24
3.3 Conclusion 30
4. FUTURE WORK 32
4.1 Limitations 32
4.2 Future Strategies 32
REFERENCES 34
BIOGRAPHICAL INFORMATION 47

LIST OF ILLUSTRATIONS

Figure Page

1.1 Illustration of the different SCI mechanisms with arrows showing general dirction of injury forces. A) contusion, B) dislocation, C) distraction, and D1) complete transection, and D2) partial transection 2

1.2 Radiographs of progressive right thoracic adolescent idiopathic scoliosis before and after rod and pedicle screw fixation. A) Preoperative standing lateral view, B) preoperative standing posterior-anterior view, C) postoperative standing lateral view, and D) postoperative standing posterior- anterior view. 5

1.3 TcMEPs recorded from right and left lower limb of a patient during corrective surgery. (A) Normal right and left TcMEPs recorded before correction forces were applied. B) Recordings disappeared immediately after a hook was inserted into the spinal canal. C) TcMEPs recovered within 2 minutes after hook removal but amplitudes still remain decreased. D) Amplitudes returned to baseline after 10 minutes. 7

2.1 Picture of overall device with computer connected 10

2.2 Machined structural components. A) Base plate with attached, B) side supports, and C) actuator bases. 11

2.3 D) Undercarriage pieces where knobs are tightened to secure actuator bases to side supports during distraction. E) Actuator connectors with Zaber actuators connected. 13

2.4 F) Guide block connected to G) guide rails. H) Supports connected at actuator tip. 15

2.5 Clean rat vertebral columns were used to prove concepts. In the first generation clamps, flexible nylon screws were used to accommodate clamping, and clamp tips were unsharpened. 16

2.6 Custom clamps connected to (J,K) clamp couplers and L) load cell. 17

2.7 Custom clamps in place around T9 and T11 just before distraction. TcMEP wires can also be seen. 19

2.8 CAD model of components needed for contusion/dislocation injuries. A) Vertical supports allow for sliding drop weights to create contusion or can be fixed for dislocation. B) Adjustable holders to accommodate injury placement. C) Coupler needed to connect forceps to actuator without side supports. 20

3.1 Left deltoid muscle (A) baseline response and (B) post-injury muscle response 24

3.2 Left gluteal muscle (A) baseline response and (B) post-injury muscle response 25

3.3 Right deltoid muscle (A) baseline response and (B) post-injury muscle response 25

3.4 Right gluteal muscle (A) baseline response and (B) post-injury muscle response 25

3.5 Quantitative evaluation of locomotor function following bidirectional distraction injury. Following a 7 mm lesion, all experimental animals dropped from a baseline BBB score of 21 (normal) to a score of 0 or 1 (little to no hindlimb movement) post-op days 1-7. This reduction shows the extreme severity of such a paradigm compared to those animals that underwent surgery and clamp positioning, but no distraction (sham operated controls). 26

3.6 Representative gross anatomical representation of the spinal cords 24 hrs. after 7mm distraction injury. A) The epicenter of the injury shows a dramatic reduction in tissue volume that gradually improves 5mm from the lesion site. B) H & E histochemistry and C) visualization of GFAP-positive reactive astrocytes confirmed the extent of the lesion at, and near to the injury epicenter. Arrows indicate the areas of decellularity. Scale bar = 3mm (A) and 500 μm (B and C)..... 27

3.7 A) Spinal cord cross sections stained for ED1, post injury tissue shows massive amounts of macrophages. B) NueN stains show obliteration of neuronal cell bodies post injury. Scale bar = 500 μm 28

3.8 A representative force over time series during distraction. A) Shows an event that increased force possibly the breaking of attached muscle or tendon. B) Peak Force recorded during distraction..... 30

LIST OF TABLES

Table Page

2.1 Calibration Test Results 18

3.1 Force Data 29

CHAPTER 1

INTRODUCTION

1.1 Incidence and Prevalence

1,250,000 Americans are currently affected by traumatic spinal cord injuries (SCI), with over 10,000 new cases occurring each year, of which 80.8% are male [1-4]. 50.9% of SCI occur between the ages of 16 and 30; the mean age being 33.7 at injury, and 19 being the most common age at injury. Motor vehicle accidents have been reported to be the most common cause of SCI (41.3-35%), followed by falls (31.1-27.3%), violence (15-5%), and sports related injuries (9.3-7.9%) [5-6].

SCIs often result in loss of function (neurological deficit, paralysis), which can result in catastrophic long-term disability and a decreased quality of life for the injured and their families. The most frequent type of paralysis associated with SCI at hospital discharge is incomplete tetraplegia (30.2%), followed by paraplegia (25.5%), complete tetraplegia (20.2%), and incomplete paraplegia (18.5%). Less than 1% of patients had complete neurological recovery at discharge [6].

Median life expectancy of persons between the age of 25 and 34 suffering from SCI was 38 years post-injury and only 43% survived at least 40 years [7-8]. Sadowsky and colleagues [9] estimate the total annual cost associated with SCI, in terms of health care utilization, rehabilitation, and loss of productivity, to be 7.7 billion dollars.

1.2 Classification of SCI

1.2.1 Primary Mechanisms

The primary mechanism of SCI is defined as the mechanical means by which the injury occurs during the initial moments of traumatic insult, and is generally categorized into 4 categories of injury: contusion, dislocation, partial or complete transection, and

distraction/flexion (Fig. 1.1). Bone fragments, disc material, and ligamentous structures can disrupt, tear, or physically obliterate axons and neurons causing neurological deficit.

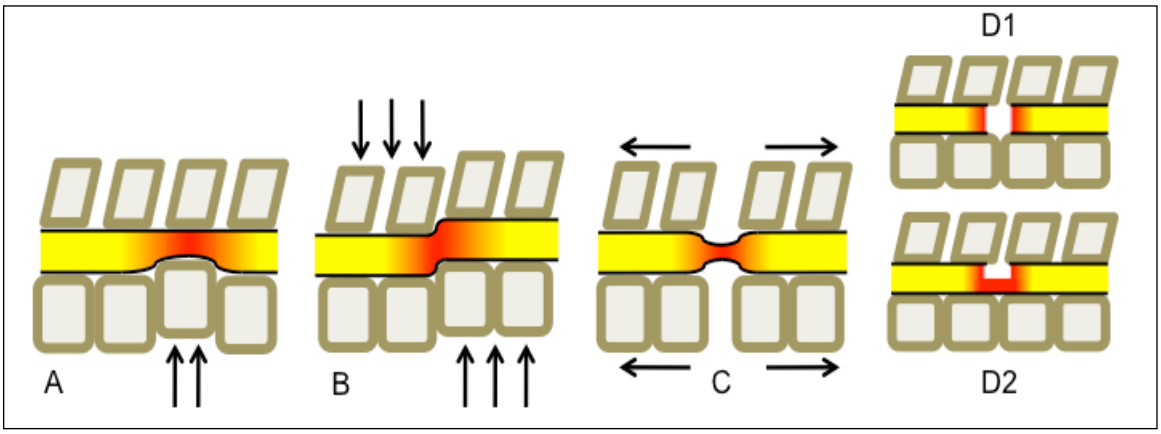

Figure 1.1 Illustration of the different SCI mechanisms with arrows showing general dirction of injury forces. A) contusion, B) dislocation, C) distraction, and D1) complete transection, and D2) partial transection

1.2.1.1 Contusion

Contusion/compression injuries occur when high-energy traumatic forces exceed the strength of bone. This causes the bone to break and sends pieces of bone into the spinal canal creating crushing, direct pressure, or ongoing compression of the spinal cord. These injures are most often caused by vertebral body fractures, which has a prevalence of 30-48% [5, 10]. Bleeding and swelling can also inflict direct destructive physical contact which can lead to neuronal death, resulting in loss of function [11].

1.2.1.2 Dislocation

29-45% of SCIs in humans are classified as dislocation injuries [5, 10], and 90% of dislocations that occur above T10 result in complete paraplegia, and 60% of dislocations occurring below T10 result in nerve damage which can lead to permanent paralysis [12]. Dislocation injuries occur when normal anatomical alignment of the spinal column becomes disrupted by displaced vertebral bodies being forced out of regular position; this sliding or slipping action of adjacent vertebral segments results in a shearing of the spinal cord.

Ligaments and/or discs connecting vertebrae can stretch or tear causing spinal instability and excessive movement between joints causing pain or damage to spinal nerves

1.2.1.3 Transection

When the spinal cord is entirely severed, via blunt trauma, immediate, complete paralysis is observed below the injury site; conversely, partial transection can lead to partial paralysis. Transection injuries are the most widely studied SCI animal model because it is simple to reproduce [13-22]. Although, a small percentage of total reported cases of SCI, violence is the leading cause of transection injuries; 21.8% resulting from gunshot wounds [23].

1.2.1.4 Distraction

Distraction injuries, also known as flexion injuries, occur when the cord is mechanically stretched. As with most materials the spinal cord will have elastic behavior, however when stretched past its limit, the cord will permanently deform causing neuronal death. Most commonly this injury is produced by a seatbelt acting as a fulcrum over which the spine is stretched in different directions [24]. Introduction of the three-point seat belt in the 1960s has helped to mitigate this type of injury in the thoracic region, however it still remains prevalent in the cervical region.

1.2.2 Secondary Mechanisms

Moreover, the initial trauma triggers a cascade of secondary biochemical and cellular events that continue to deleteriously affect neurons after the primary injury. These include: 1) Loss of microcirculation, ischemia, and hemorrhaging, often leading to sensory and motor neuron cell death (necrosis) by depriving cells of essential nutrients provided by the blood [23, 25-27]. 2) Free radicals, having unpaired electrons, have the ability to disable vital molecules necessary for cell function [28-31]. 3) In another response to injury, neurons flood the site with glutamate, and excessive levels of glutamate have been shown to cause excitotoxicity; killing neurons and protective oligodendrocytes [32-34]. 4) Another secondary mechanism involves the inflammatory response by the immune system, which combats infection by restricting damage

and begins tissue repair. The immune response also increases the expression of the transforming growth factor-beta (TFG-β) that triggers reactive astrocytes to increase the secretion of chondroitin sulfate proteoglycans (CSPGs), which in turn are inhibitory for axonal regeneration [35-38]. 5) SCI has been shown to initiate apoptosis, another secondary mechanism, which is programmed cell death used by the body to get rid of old and unhealthy cells [39-41]. These secondary mechanisms exacerbate the primary insult by further damaging cells and/or by obstructing neuronal regeneration which impedes the ability of neurons to transmit information to and from the brain.

1.2.3 Current SCI and Neuronal Repair Treatment

Many strategies for SCI treatment have been explored and include: oxidative stress reduction by free radical inhibition [42], blood flow management [43-44], inflammation attenuation [45-47], and blocking glutamate receptors for excitotoxicity prevention [48-50]. Initially, methylprednisolone [51-52] was the most widely accepted treatment for clinical use, however it remains controversial [53-55]. Still, no single treatment has proven successful in treating SCI

1.3 Scoliosis

Scoliosis is a complex, structural spinal deformity of three-dimensions involving lordosis, lateral deviation, and axial rotation [56-57]. Scoliosis is caused by genetic or idiopathic disruptions that result in the progressive curvature [58-59], however the exact aetiopathogensis of this deformity still remains unclear [60-61]. Of every 1,000 children, 3-5 will develop adolescent idiopathic scoliosis [62]. The most at risk population group for idiopathic scoliosis is adolescents from 10-16 years of age, and in the general adult population, prevalence of scoliosis has been estimated to be anywhere from 2-32%, more specifically 20% among the elderly [63-67].

Adams' forward bend test and a scoliometer are used for quick screening of patients however, definitive diagnosis is made by measuring the Cobb angle taken from radiographs [67]. The Cobb angle is the angle between the uppermost and lowest inclined vertebra, and Cobb angles of 45° or more are considered to be clinically severe [68]. Backache or pain, fatigue, and

uneven shoulders or hips are symptoms of scoliosis, and severe cases of scoliosis can compromise respiratory function and could result in mortality. If detected early scoliosis can usually be stabilized and blocked from further progression using non-surgical methods such as bracing or halo-femoral traction. Braces are rigid, closefitting, supportive devices that are applied around the torso/trunk of a patient. Halo-femoral traction involves a halo, anchored to the skull of the patient, connected to femoral pins; weights are then added to provide traction. More severe cases of scoliosis exhibit visible rib 'hump' (hunchback), which can have detrimental psychosocial outcomes on those it affects, especially since the populations most affected are those in puberty. Furthermore, treatment with bracing is uncomfortable and minimally discrete to peers [69-71].

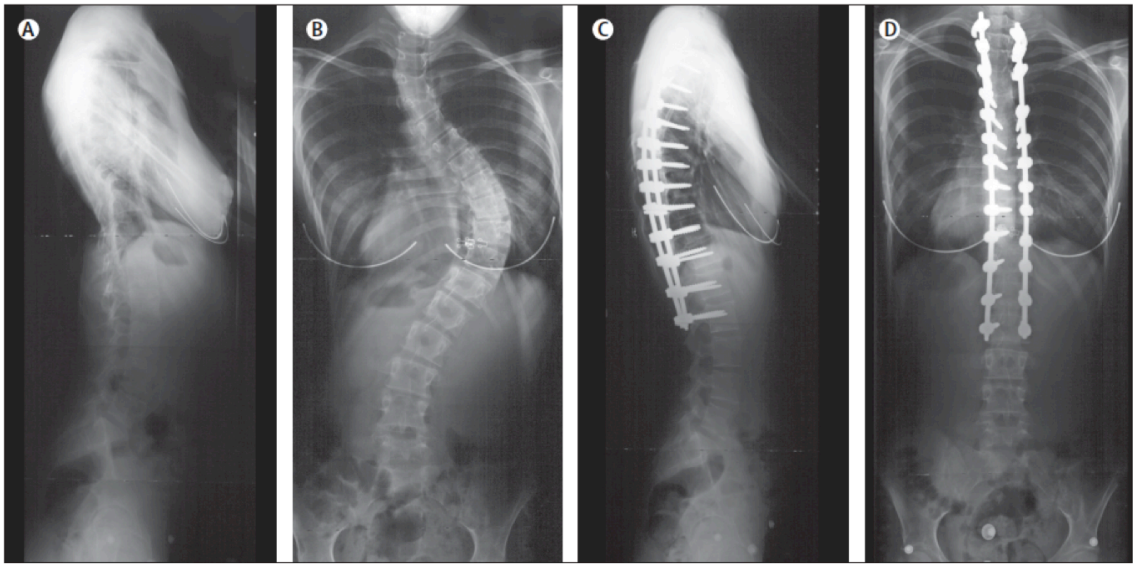

Figure 1.2 [57] Radiographs of progressive right thoracic adolescent idiopathic scoliosis before and after rod and pedicle screw fixation. A) Preoperative standing lateral view, B) preoperative standing posterior-anterior view, C) postoperative standing lateral view, and D) postoperative standing posterior- anterior view.

Severe cases of deformity are routinely surgically corrected. This procedure involves the placement of rods, used to straighten the vertebral column, fixed to screws that are secured into vertebral pedicles (Fig. 1.2). In order to maximize curvature correction, surgeons take

advantage of viscoelastic properties of the spine by applying traction/distraction forces intraoperatively. This can be done by application of small amounts of temporary internal distraction, using the newly installed implant hardware and instrumentation [72-73]. Another method surgeons implement is to place a halo on the patient's head and a brace on the leg, and distraction is induced when a gentle pulling force is applied (personal communication with Dr. Daniel Sucato).

The correction forces used during surgery produce significant multidirectional stress to the spinal cord; which in severe cases can damage the spinal cord resulting in a new neurological deficit, the most feared risk of scoliosis correction [74-76]. Recently the total incidence of neurological deficits for surgical correction of scoliosis was found to be 1.89% [77], but reports range from 0.7%-2% [78-79]. Most deficits were found to be transient or mild, moreover incidence of severe or permanent deficit was reported to be only 5.3% of total incidence [80].

1.3.1 Intraoperative Prevention Against Deficit

In order to reduce, detect and alert surgeons to devastating neurological deficit during deformity correction surgery, as quickly as possible, the highest standard of care involves intraopertative neurological monitoring [81]. One type of intraoperative monitoring is somatosensory-evoked potentials (SSEPs), which are elicited by electrical stimulation of a peripheral nerve, and responses are recorded above and below the surgical site repeatedly during the procedure. Based on significant changes compared to a baseline taken before surgery, functional status of the sensory tracts can be evaluated. Another method of intraoperative monitoring is transcranial motor-evoked potentials (TcMEPs). The motor cortex of the patient is electrically stimulated and responses in major muscles above and below the surgery site are recorded. If nerves of the spinal cord are injured during surgery, recordings will show a reduced or lack of response from their target muscles below the surgery site (Fig. 1.3). By using a combination of SSEPs and TcMEPs monitoring, surgeons are able to better manage the risk of neurological deficits [82-84].

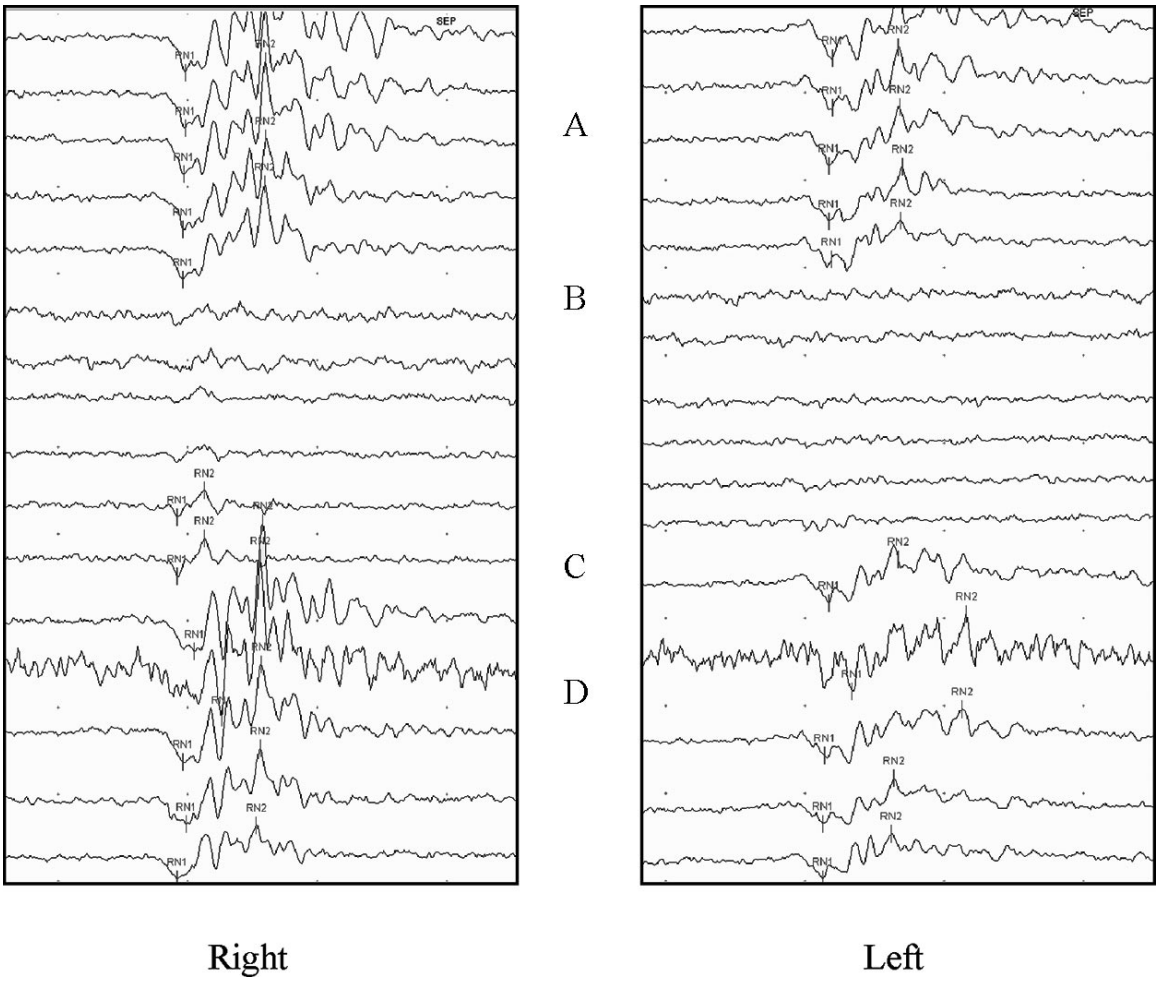

Figure 1.3 [85] TcMEPs recorded from right and left lower limb of a patient during corrective surgery. (A) Normal right and left TcMEPs recorded before correction forces were applied. B) Recordings disappeared immediately after a hook was inserted into the spinal canal. C) TcMEPs recovered within 2 minutes after hook removal but amplitudes still remain decreased. D) Amplitudes returned to baseline after 10 minutes.

1.4 Animal Models

The evaluation of therapeutic approaches to all SCIs is normally tested using animal models. Current animal models can be divided into simple and complex models, according to the types of injury that can be induced.

1.4.1 Simple Models

A commonly used simple model of SCI is contusion. Alfred R. Allen in 1911 described the first contusion SCI animal model by dropping a weight on to the spinal cord of a dog [86]. The

weight-drop method of creating a SCI, since then, has become the most widely accepted, clinically relevant animal model for contusion SCI [87-91]. Specifically, the NYU-MASCIS impactor model has been able to standardize mild to severe contusive injuries by the variation of height at which the weight is dropped.

Transection animal models are currently the most commonly studied, especially in the investigation of neural regeneration. The injury is easy to create and is done by severing the cord with a blade or micro scissors. However, the regenerative and neural protective strategies that are derived from these studies are constrained to minimal clinical relevance because of the very low prevalence of these types of injuries [4, 92-93].

1.4.2 Complex Models

Animal models for vertebral dislocation include those reported by Fiford et al. [94] and Choo et al. [4]. The device created by Choo et al. uses small scale custom fabricated clamps that attach around lateral processes of different cervical vertebral bodies. Once secured, the rostral clamp remained stationary while the caudal clamp was dorsally translated to create a shearing of the cord.

Attempting to reproducibly create distraction SCI, Choo et al. created a distraction injury by placing clamps tightly around cervical vertebra; the rostral clamp remained stationary, while a linear actuator pulled the other clamp caudally. This distraction injury was unilateral meaning one clamp was held stationary while the other clamp was pulled by a linear actuator. Behavioral confirmation of injury was not investigated so injury reproducibly could not be assessed.

To date one animal model has attempted to create bi-dirctional distraction injury as seen in scoliosis corrective surgery Dabney et al. [95] used modified Harrington hooks placed sublaimarly at T9 and T11. The hooks were connected to a stepper motor that displaced the hooks in opposite directions. However, results were highly variable; following a 7mm distraction 3 of 8 animals showed no behavioral abnormalities, while the remaining 5 had inconsistent

degrees of injury severity. Additionally, to accommodate sublaminar hook placement, a partial laminectomy is required which can lead to direct traumatic insult to the cord.

This model cannot replicate the bi-directionality of distraction injuries that are present in most cases of SCI during scoliosis corrective surgery. Therefore, we hypothesize that with a computer controlled device, bi-directional distraction injuries can be predictably reproduced.

1.5 Project Aims

Currently there is no reliable animal model that can mimic spine deformity correction surgery. The establishment and characterization of such model would allow for in-depth investigation of neuroregenerative and neuroprotective strategies that would benefit and protect future persons, who suffer with spine deformity, through neurological deficit prevention. Specifically the aims of this project are:

1. Design, fabricate, and test a novel device for the controlled and reproducible damage of the spinal cord through bidirectional spine distraction in rats.
2. Using a 7mm distraction injury, document intraoperative Transcranial Motor Evoked Potentials (TcMEPs)
3. Characterize the functional deficit of the distraction injury through behavior testing
4. Evaluate the extent of tissue damage using histological and immunocytochemical methods.

CHAPTER 2

DESIGN AND FABRICATION OF UTA DISTRACTOR DEVICE

2.1 Design Requirements

In order to create and characterize a reliable animal model that simulates neurological deficit that can occur during spine deformity correction, the following design requirements must be met: 1) injuries that are induced must be reproducible, 2) device must accommodate the monitoring of SSEPs and TcMEPs, 3) distraction must be bi-directional to simulate forces present during scoliosis surgery, 4) allow for long-term survivability of the rat for injury characterization, 5) device must easily accommodate all sizes of rats, and 6) any interaction between the device and animal must be biocompatible.

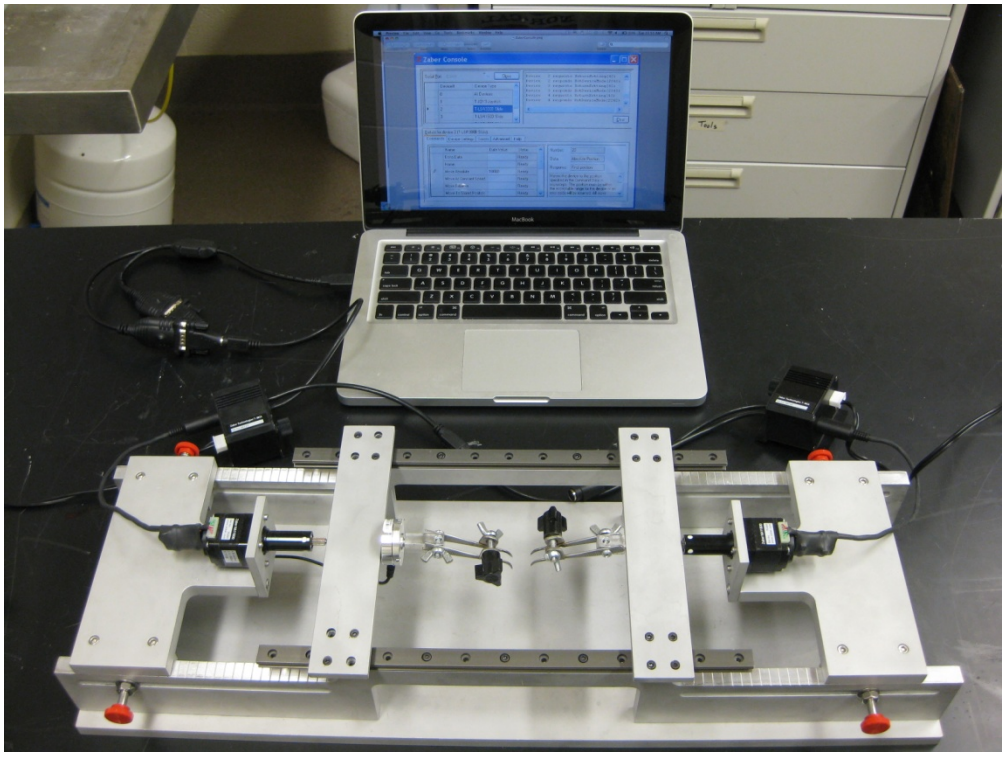

Figure 2.1 Picture of overall device with computer connected.

2.2 Design Details

The device (Fig. 2.1) is 24 inches long, 8 inches wide, stands 4.75 inches tall, and weighs approximately 25 pounds; it fits in any small laboratory space and can be easily transported. The 5 main components of the device are: 1) machined structural components, 2) linear actuators, 3) supports and guides, 4) load cell, and 5) custom clamps.

2.2.1. Structural Components

All structural components were machined from aluminum alloy 6061. This material was selected for its high yield strength (40,000 psi), ease of machinability, and relatively inexpensive cost. All parts were machined at UTA by the UTA Physics Machine Shop.

2.2.1.1 Base Plate

The base plate (Fig. 2.2, A) measures 24 inches long, 8 inches wide, and .375 inches thick. 16 counter-sunk holes were placed in the base plate for connection to side supports, which makes the entire device very sturdy and durable.

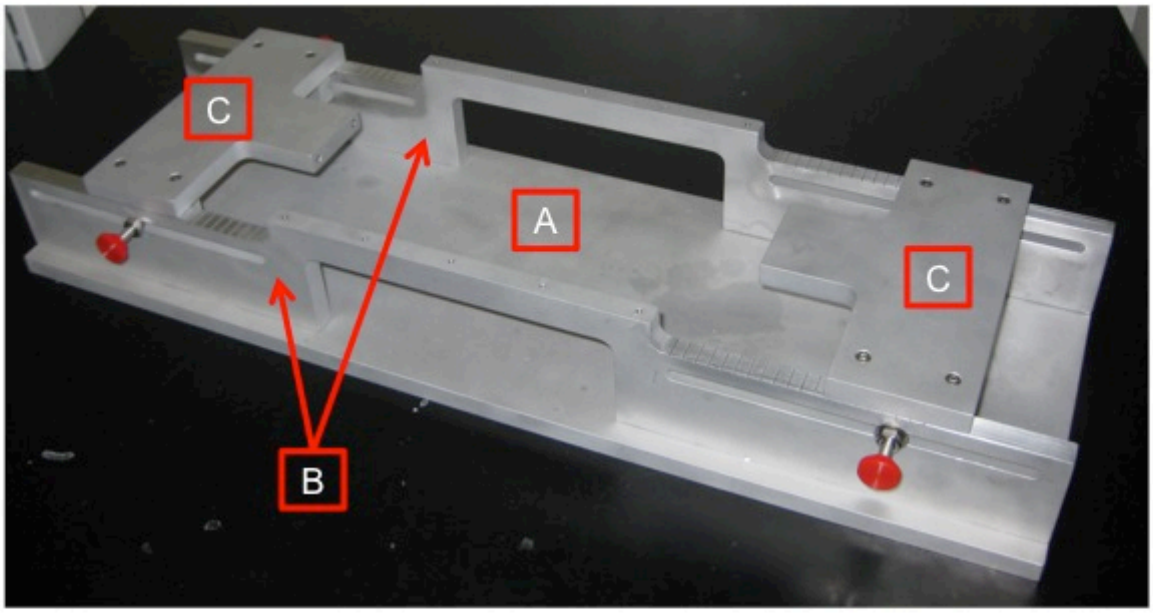

Figure 2.2 Machined structural components. A) Base plate with attached, B) side supports, and C) actuator bases.

2.2.1.2 Side Supports

Side supports (Fig. 2.2, B) are ½ inch thick pieces that span the entire length of the device. They are 2.90 inches tall and placed 6 inches apart which offers generous amounts of space to accommodate all rat strains that may be used. Additionally, it was designed to provide plenty of room for SSEP and TcMEP wiring and other equipment that the user may want to use, such as additional stereotaxic equipment. A 7 in. x 2.25 in. rectangular cut out was placed in each side support for easy access to the animal and equipment in use during the distraction protocol.

The raised portions of the side supports have 5 tapped holes for guide rail placement (Fig. 2.4, G). Along the top of the lower portions, etched markings were placed every ¼ inch to help with consistent sliding base placement during distraction. 2-6¾ inch long slots were placed in each side support ½ inch from the end of each piece to facilitate the sliding and locking action of the sliding bases.

2.2.1.3 Sliding Bases

Sliding bases (Fig. 2.2, C) are 7 inches wide and .48 inches thick, and held to a ±.005 inch flatness tolerance which helps the pieces slide evenly over the side supports when being moved into position by the operator. Each sliding base has 2 undercarriage pieces (Fig. 2.3, D) attached .75 inches from the edge to its underside, and this creates a lip so that it fits in between and on top of the side supports. The undercarriages have a threaded hole placed through the entire piece that lines up with the slot cut out of each side support where a knob is inserted. This serves to lock down the sliding base once clamps are in place and animal is ready to be distracted. The sliding feature of this device enables the user to easily place and adjust clamp placement depending on animal size, anatomy, or desired distraction location. Actuator connectors (Fig. 2.3, E) were vertically attached to the end of each base for actuator connection.

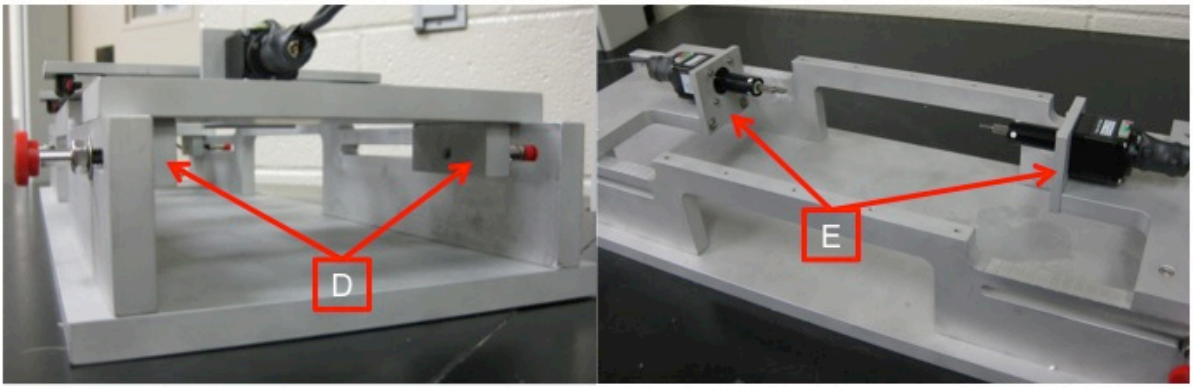

Figure 2.3 D) Undercarriage pieces where knobs are tightened to secure actuator bases to side supports during distraction. E) Actuator connectors with Zaber actuators connected.

2.2.2. Actuators

In order to produce bidirectional distraction injuries, 2 electric actuators were mounted to the actuator connectors exactly opposite each other. The Zaber Technologies' electric NA11B30 actuator was chosen for the following reasons: 1) each actuator has 80 Newton pull capacity. Current studies have shown the force needed to distract to be approximately 40 N [96], and these particular actuators allow for a twice the needed force (safety factor of 2). 2) Actuators each have a 30 mm travel distance. The distance needed to create a severe injury in a rat has been hypothesized to be 7mm, 3.5mm in each direction from the midline [95]. These actuators allow for a total of 60 mm of bidirectional distraction distance extending the ability to characterize injuries at varying lengths of distraction. 3) Actuators have an accuracy of +/- 8μm and repeatability of < 0.4μm. These specifications tightly limit the possibility of variation of results due to variations of distraction distance. 4) A maximum speed of 20 mm/s and a minimum speed of 0.0009302 mm/s. This allows the user to experiment and characterize injuries at different speeds. Slower speeds would more closely represent spine deformity correction, whereas higher speeds could be used to simulate trauma from falls and motor vehicle accidents. 5) User-friendly software helps to simultaneously control both actuators in a bidirectional manner.

2.2.2.1 Actuator Controllers

Each actuator was connected to a stepper motor controller (Zaber Technologies T-MCA) that offers microstepping for precise control of linear actuators, manually or through computer software. Controllers were daisy chained together and a serial to USB adapter was used to link into a computer.

2.2.2.2 Actuator Software

Zaber Console Software package was provided by Zaber Technologies and is extremly user-friendly. Settings such as distance, speed, acceleration, and microstep size were all defined and controlled by the console. This software could be programmed to induce bi-directional injury by having each actuator retract half the total distraction distance i.e. 7mm total; each actuator moves 3.5mm. Controllers and software helped keep distance, speed, and acceleration variables constant throughout experiments greatly increasing the ability of the animal model to consistently reproduce computer controlled distraction injuries.

2.2.3. Supports and Guides

Supports (Fig. 2.4, H) had threaded holes placed in the center of their thickness for threaded actuator tip connection on one side and clamp or load cell coupler on the opposite side. At each support end, guide blocks (Fig. 2.4, F) were secured, and accompanying guide rails (Fig 2.4, G) were attached to the top of each side support. Actuator supports are also designed to counter the bending moment that would exist due to the weight of clamps, clamp connectors, and load cell if connected directly to the tip of the actuator. Additionally guide blocks and rails assure maintenance of a linear, bi-directional motion during distraction.

PBC Linear's Mini-Rail Sigma guides and rails were specifically selected for the following reasons: 1) 0.1-0.2 coefficient of friction allows for more accurate force reading during distraction. 2) Parts are made of corrosion-resistance material that protects blocks and rails from damage in a surgical environment. 3) A max speed 10m/s is sufficient to handle the maximum possible speed of the actuators during experimental testing. 4) Rails and block are

rated at 10,000 psi which is very capable of handling comparatively small forces created during distraction. By incorporation of a support and guide system, possible inconsistencies of injury results due to non-linearity or bending were suppressed.

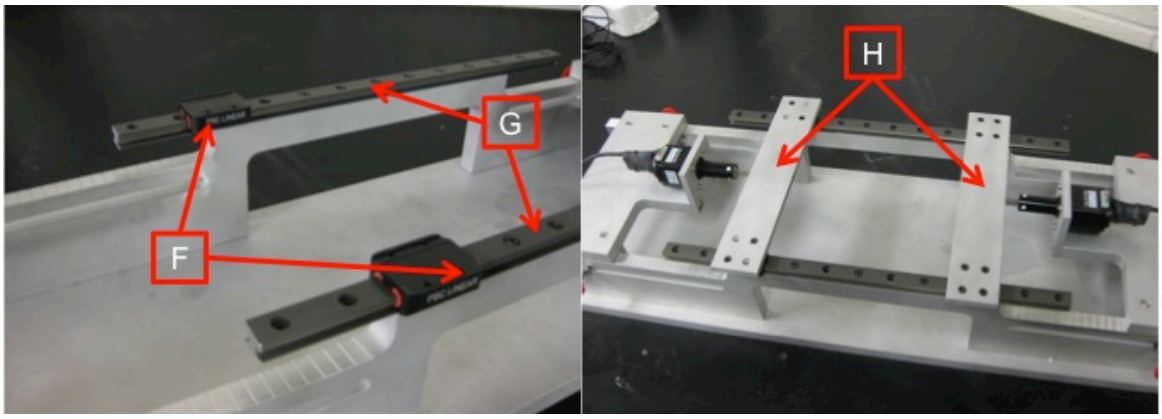

Figure 2.4 F) Guide block connected to G) guide rails. H) Supports connected at actuator tip.

2.2.4. Load Cell

An iLoad Mini load cell (Fig. 2.6, L) by Loadstar Sensors was chosen to record distraction forces for the following reasons: 1) 1.0% accuracy of full scale will give sufficient force readings during distraction. 2) Low profile makes it is easily attachable to actuator supports and does not interfere with any surgical procedures. 3) Current studies have shown the force needed to distract to be approximately 40 N [96], which is equivalent to about 9 lbs. This load cell has a 0-20 lb. capacity leaving plenty of cushion room if forces are higher than expected. 3) 3kHz, 3000 samples per second, sample frequency will ensure major forces during distraction are recorded. 4) Relatively inexpensive and easily connects to USB port, which cuts down on human or mechanical error that can occur during instrumentation programming, amplifying, etc. 5) User friendly software, LoadVue, records and logs distraction forces to a data file.

2.2.5. Custom Clamps

The most critically important, and most difficult, aspect of the device was the clamping strategy. To generate ideas and for proof of concept of acceptable clamping methods, rat

spinal columns were extracted and all muscle and tissue was removed from the vertebra (Fig. 2.5). Initially one idea was to have clamps that would tighten around the respective dorsal processes of the vertebra, however the processes proved too weak to withstand the load of distraction forces and processes broke off or were crushed during testing. Finally an acceptable method was chosen by which the vertebral body would be clamped to bear the majority of distraction forces while the tips of the forceps would be placed in front of transverse processes for added support. Slippage off the vertebral body was insignificant with the use of forceps with serrations.

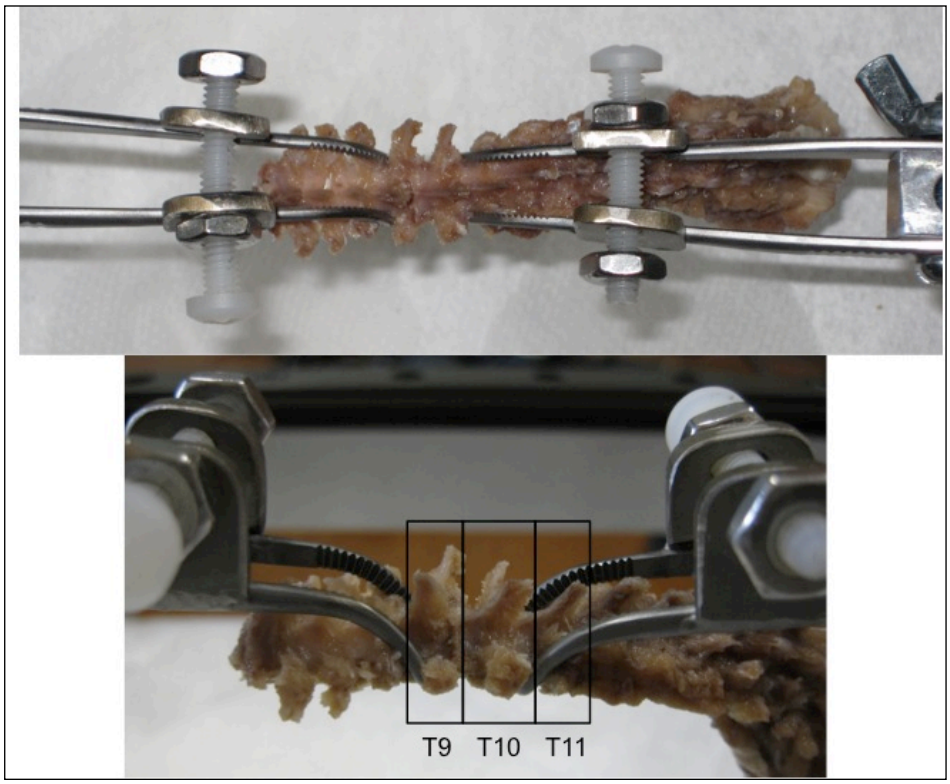

Figure 2.5 Clean rat vertebral columns were used to prove concepts. In the first generation clamps, flexible nylon screws were used to accommodate clamping, and clamp tips were unsharpened.

Custom clamps were constructed from Fine Science Tools' narrow patterned curved forceps (11003-12). Forceps were separated and each piece cut to a 3-inch length from the tip. A ¼ inch hole was placed through the end for attachment to clamp couplers (Fig. 2.6, J and K).

Each piece had a ½ in. x ½ in. x .1 in. flange, with threaded hole, laser welded to the outside starting .100 inches from the end of the tip serrations. Using a screw and wing nut clamp, pieces were tightened to clamp couplers already firmly attached to actuator supports. A flexible, nylon screw was threaded through the flanges to used to close the clamps (Fig. 2.5).

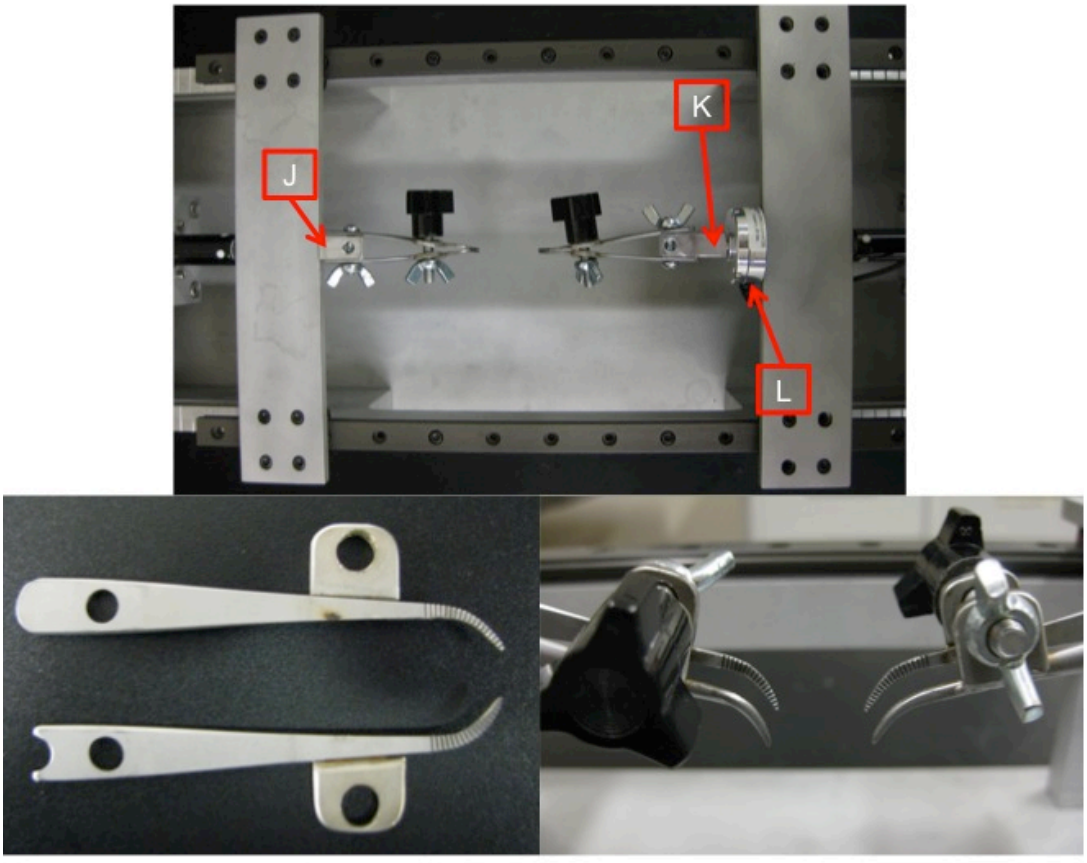

Figure 2.6 Custom clamps connected to (J,K) clamp couplers and L) load cell.

2.3 Bench Top Testing

To assure a distance of 7 mm was achieved the actuators were calibrated. This resolved distance error due to micro step truncation entered into computer program and any play that existed between actuator, supports, couplers, and clamps. Pins were attached to the tips of the clamps and the distance between the pins measured using a caliper. Actuators were programmed to move 7mm, and the final distance from pin to pin was recorded. This process

was repeated 10 times. Repeatability, or the deviation in actual final position when repeatedly instructing the device to move 7mm from the same direction, was 10μm (Table 2.1). Zaber specifies the repeatability of the actuator to be <0.4μm, however we did not have technology to measure at that resolution.

Table 2.1 Calibration Test Results

Trial	Measured Distance (mm)
1	7.00
2	7.00
3	7.00
4	7.01
5	7.01
6	6.99
7	7.00
8	7.00
9	7.01
10	7.00
Average	7.00
Standard Deviation	0.01

The objective of the initial experimental testing was to distract a distance of 7mm, a distance classified as causing a severe injury in the work by Dabney et al. [95]. However, during the initial test clamps were unable to be properly secured around the vertebral body when tightened and the test was terminated.

During this first attempt at distraction it was discovered that during tightening of the clamps, each side of the clamp did not line up exactly with its counterpart, making it impossible to grip around the vertebral body with confidence. When the parts of the clamp and clamp coupler were examined it was determined to be a result of holes in the side of each clamp piece

not being placed in the exact same location, and the solution was to simply rework the holes so that each clamp side would line up exactly together when tightened all the way closed.

During the next attempt at a 7mm distraction, clamps slipped off the vertebral body during distraction, therefore there was no actual distraction of the spinal cord. Slipping of the clamps during this second test revealed that the nylon screw used could not be easily tightened by hand to provide sufficient gripping strength. Flange threads were ground out and the size of the hole increased to accommodate a knob and wing nut for better gripping strength. It was also observed as the clamps slipped that they were not placed deeply enough to hook around transverse processes. Forceps tips were sharpened for easy penetration of any remaining connective tissue between vertebra and transverse processes that was not removed during surgical procedures (Fig. 2.7). After the described fixes were made to the device, the first successful distraction took place in January.

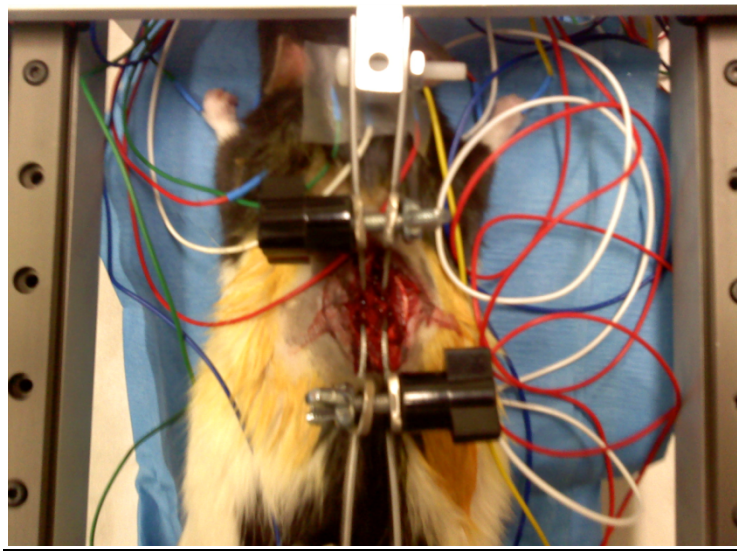

Figure 2.7 Custom clamps in place around T9 and T11 just before distraction. TcMEP wires can also be seen.

2.4 Future Device Modifications

For current research purposes, only the components necessary for distraction injury were manufactured and assembled. Furthermore, during the development of the device,

additional components were designed and modeled to easily allow for the creation of contusion and dislocation SCIs as well (Figure 2.8). Currently there is no single device on the market capable of offering researchers the ability to reliably create all three of the most common SCIs studied. The contusion/dislocation components have not yet been fabricated and injury reproducibility has not been experimentally tested. However, we believe this versatile device will offer highly reproducible injuries for further animal model characterization and efficient screening of present and future SCI treatment.

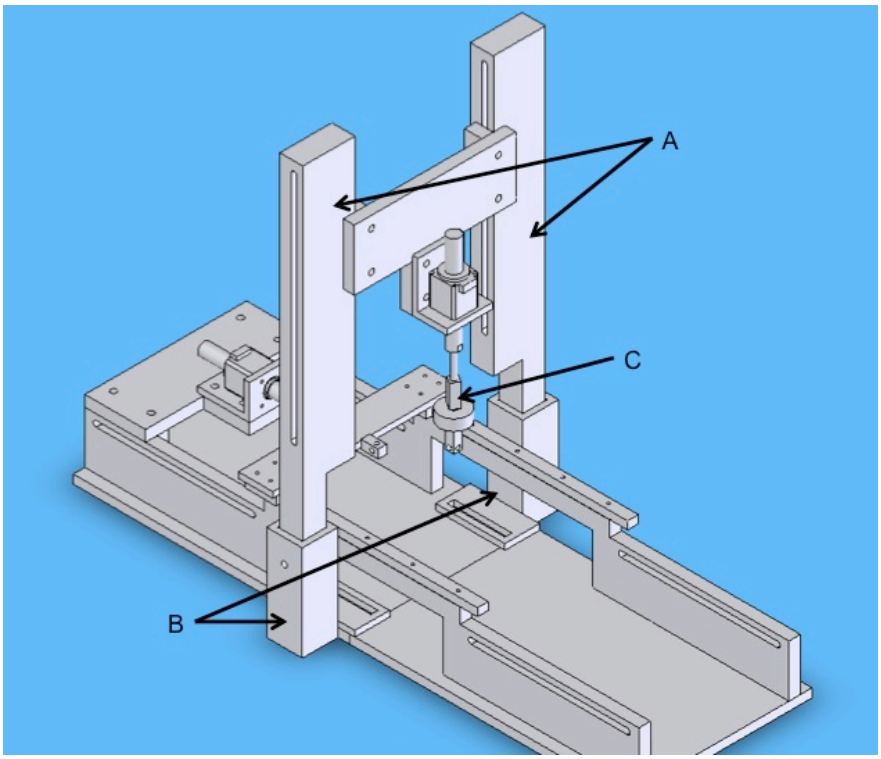

Figure 2.8 CAD model of components needed for contusion/dislocation injuries. A) Vertical supports allow for sliding drop weights to create contusion or can be fixed for dislocation. B) Adjustable holders to accommodate injury placement. C) Coupler needed to connect forceps to actuator without side supports.

CHAPTER 3

EXPERIMENTAL DISTRACTION INJURY

3.1 Methods

3.1.1. Device Preparation

Before animal preparation began, computer controlled equipment was tested to confirm that it was functioning properly. Actuators settings, such as speed, acceleration, distance, and microstep size, were verified through Zaber software, and the load cell was calibrated and re-calibrated after manual tension was applied to ensure recording software was logging data.

3.1.2. Animal Procedure

Six female Long-Evans rats (275-325 g) were anesthetized with sodium pentobarbital (50mg/kg) via injection into the intraperitoneal space. Once an adequate depth of anesthesia was assessed by loss of a corneal reflex, their backs were shaved and cleaned with povidone-iodine. After animal preparation was completed and subdermal needle electrodes (Cardinal Health, Dublin, OH) were placed in the rat, baseline recordings were captured before operation and placement into the distraction device. Two electrodes were placed over the motor cortex for stimulation, and recording electrodes where placed in the right and left deltoid and gluteal muscles. Reference electrodes were inserted in all four paws and a ground electrode was placed in the ventral thigh. The Cadwell Cascade™ system was used to evoke motor activity by applying three stimulation pulses (6-8V amplitude, 50μs duration, and 2-ms interval) over the primary motor cortex. TcMEP signals were recorded at a rate of 21,500 samples per second. Low (lower than 100 Hz) and high (higher than 2kHz) frequency components were filtered out, and the rest was amplified, processed, and stored by the Cadwell system.

The vertebral column was exposed by dissection of the paraspinous muscles and transection of the interspinous and facet capsular ligaments. The rat was then placed in the distraction device with its front half placed on a small platform to elevate the distraction site for clamp placement. The rostral clamp was first positioned and hand tightened around T9, and the sliding base was locked down. The caudal clamp was then secured around T11. To assure that 7mm of linear distraction would be achieved, any elasticity or play in the spine was eliminated by the application of gentle tension. This was accomplished by moving the cadual sliding base slightly back once both clamps were firmly attached. After minor tension was applied, the load cell was zeroed. Before distraction, TcMEP recordings were again taken to verify that SCI had not taken place during surgery or clamp placement procedures.

The computer program controlling the actuator distance was re-checked for correct distance input, each actuator was programmed to retract 3.5mm, a total distance of 7mm at 1mm/sec, and then executed. After actuators had stopped, another round of TcMEP data was again collected. Once the clamps were carefully loosened from the vertebral bodies and the animal removed from the device, another set of TcMEP data was recorded.

Muscle layers were approximated using chromic gut sutures and the skin was stapled. Animals received cephazolin (5 mg/kg, IM) at 4, 24, 48, and 72 hours after surgery and buprenorphine (0.05-0.1 mg/kg, SC) for pain control. All surgical procedures were performed in accordance with the guidelines of the Institutional Animal Care and Use Committee of the University of Texas at Arlington.

3.1.3. Behavioral Analysis

Open field locomotor scores are powerful tools in the evaluation of the outcomes of SCI. Tarlov and Klinger [98] developed the original open field locomotor scoring scheme in 1954, which consisted of five functional levels categorized by specific behaviors correlated with recovery. However, this test very subjective because of operationalized terms such as “good movement” or “complete recovery”.

Therefore in order to conduct more accurate, unambiguous behavioral analysis for motor function, the Basso, Beattie, Bresnahan (BBB) rating scale was used [98-99]. This 21-point scale rates parameters such as joint movements, the ability for weight support, limb coordination, foot placement, and gait stability. A score of 0 is given if no observable hind limb movement exists; however, points are accumulated for isolated joint movements, plantar placement of the paw, weight support and coordination between forelimb and hindlimb. When more joints show movement or when the movements are more extensive, the BBB score increases, and final points are achieved by toe clearance, trunk stability and tail position. Behavioral baselines were established 7 days prior to injury, and behavior was assessed each day for 7 days post injury.

3.1.4. Histology

Animals were allowed to recover for 7 days. All animals were then perfused transcardially with 4% paraformaldehyde. Spinal cords were carefully harvested, fixed overnight and processed for paraffin embedding. A 15mm section of spinal cord was isolated and divided in to 3 sections; a 5mm section proximal to the injury site, a 5mm section containing the injury epicenter, and another 5mm section distal to the injury. Embedded spinal cord sections were cut transversely and stained accordingly.

In order to observe general morphology of spinal cord structure, tissues were stained with hematoxylin and eosin (H&E) using standard protocol. To identify neuronal cell bodies present in the spinal cord, immunocytochemistry for neuronal nuclei (NeuN) staining was done. Samples were deparaffinized and blocked with endogenous peroxidase with 3% H2O2 for 10 minutes, rinsed and then blocked in universal blocking solution (Biogenex; San Ramon, CA) for 10 minutes. Slides were incubated in primary antibody overnight at 4°C (NeuN;1:200 Mouse anti-NeuN; Millipore, Billerica, MA), rinsed with tris-buffered saline then incubated with secondary donkey anti mouse antibody for one hour at room temperature (1:500; Jackson ImmunoResearch; West Grove, PA). Immunodetection of this marker was visualized by DAB

(Dako, Carpinteria, CA) used as an HRP substrate following a 30 minute incubation with peroxidase conjugated streptavidin (Jackson ImmunoResearch; West Grove, PA).

Using the same protocol mentioned above, spinal cords were also probed for reactive astrocytes using glial fibrillary acidic protein (GFAP;1:500 Mouse anti-GFAP; Dako, Carpinteria, CA) and macrophages using ectoderma dysplasia 1 (ED1;1:200 Mouse anti-CD68; AbD Serotec, Raleigh, NC) in order to more fully understand and evaluate the injury.

3.2 Results and Discussion

TcMEP data was successfully recorded before and after distraction (Fig. 3.1-3.4). Deltoid muscle recording sites (controls) showed no loss of function, which was expected because the deltoid muscles are located proximal to the injury site. However, gluteal muscle, located distal to the injury site, recordings showed significant (>75% drop in amplitude) reduction from baseline. These recordings along with postoperative behavior data, support the ability of intraoperative MEP recordings to alert surgeons to possible neurological deficit during corrective surgery.

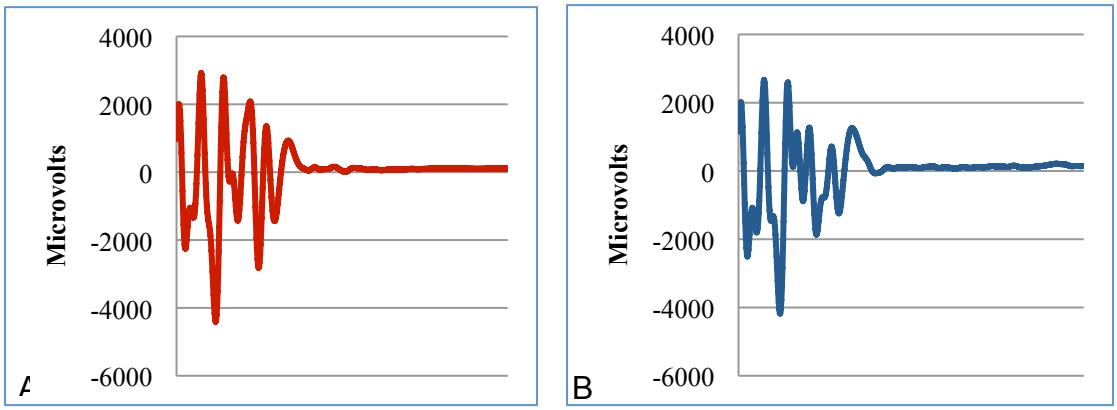

Figure 3.1 Left deltoid muscle (A) baseline response and (B) post-injury muscle response.

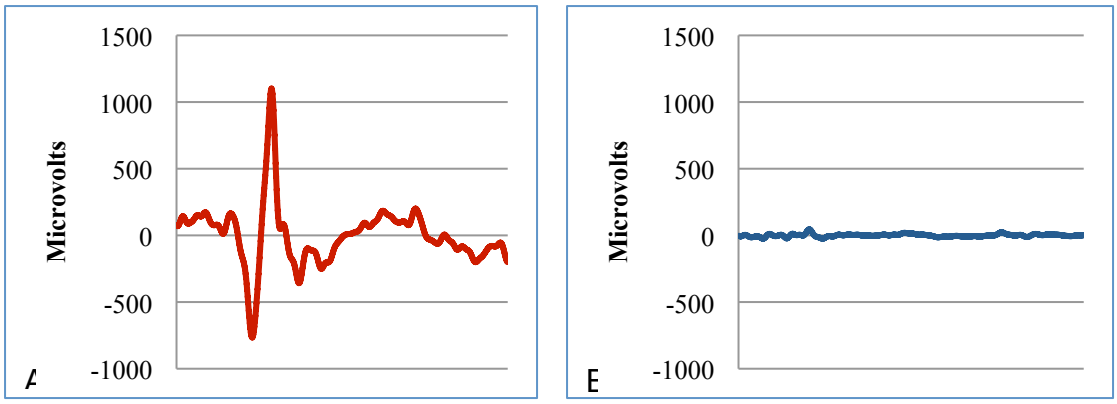

Figure 3.2 Left gluteal muscle (A) base line response and (B) post-injury response.

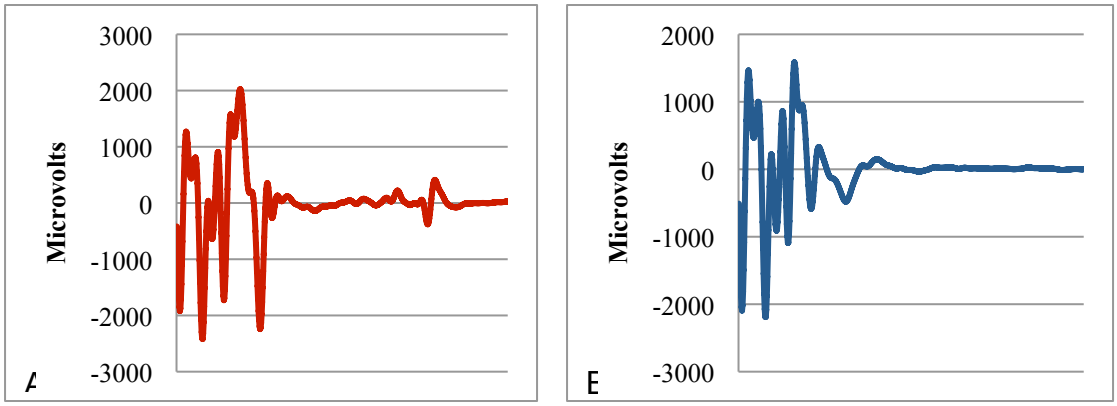

Figure 3.3 Right deltoid muscle (A) baseline response and (B) post-injury muscle response.

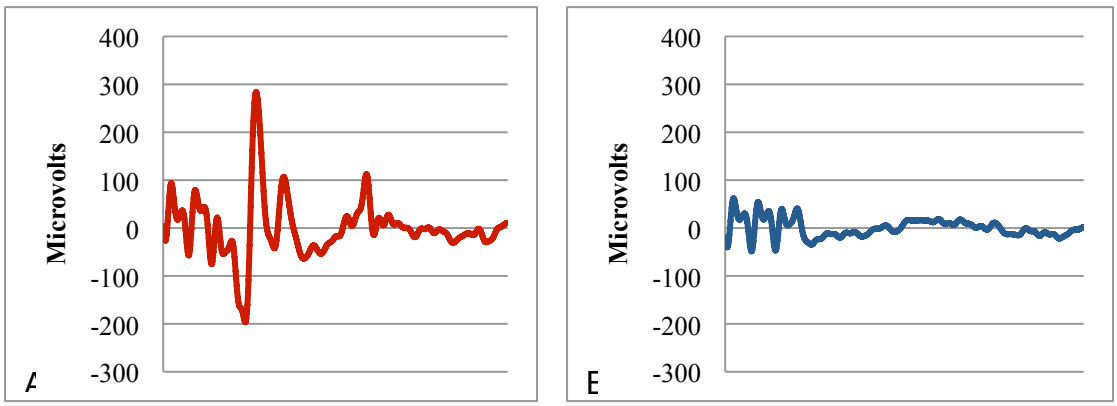

Figure 3.4 Right gluteal muscle (A) baseline response and (B) post-injury muscle response.

The 7 mm distraction of the rat spinal cord produced a clear, visual displacement of the vertebrae in both directions and reproducibly exposed the spinal cord, which indicated the severity of such distraction paradigm. The functional deficit caused by the distraction injury was highly reproducible, drastic and permanent in which none of the animals exhibited hind limb movements (Fig 3.5). All animals showed a dramatic reduction from a normal BBB locomotion

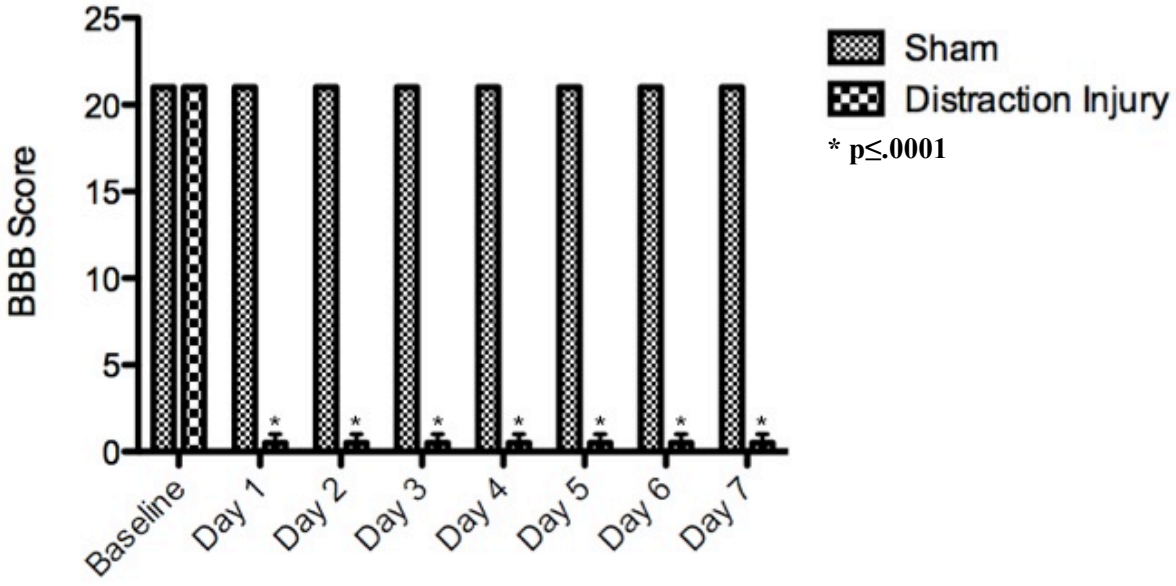

Figure 3.5 Quantitative evaluation of locomotor function following bidirectional distraction injury. Following a 7 mm lesion, all experimental animals dropped from a baseline BBB score of 21 (normal) to a score of 0 or 1 (little to no hindlimb movement) post-op days 1-7. This reduction shows the extreme severity of such a paradigm compared to those animals that underwent surgery and clamp positioning, but no distraction (sham operated controls). *p≤.0001

score of 21 prior to distraction, to a significantly lower score of 0 or 1 seven days post injury (0.17 +/- 0.41; p≤.0001). This dramatic loss of motor function and absence of any functional recovery indicates severe damage to the spinal cord due to the 7 mm distraction. These results contrast that of previous reports in which a similar distraction paradigm using modified Harrington hooks produced a highly variable injury with no functional deficit observed in some animals, in which the variability of injury reached 50%. The distraction device here reported showed a variability of approximately 5%, that is, a 10-fold improved performance over other methods [95]. The linearity of the applied forces and the bidirectional distraction in the reported

device seemed to have contributed to the enhanced reproducibility of the injury and to have induced more severe damage to the spinal cord compared to other methods [4, 95, 96, 100].

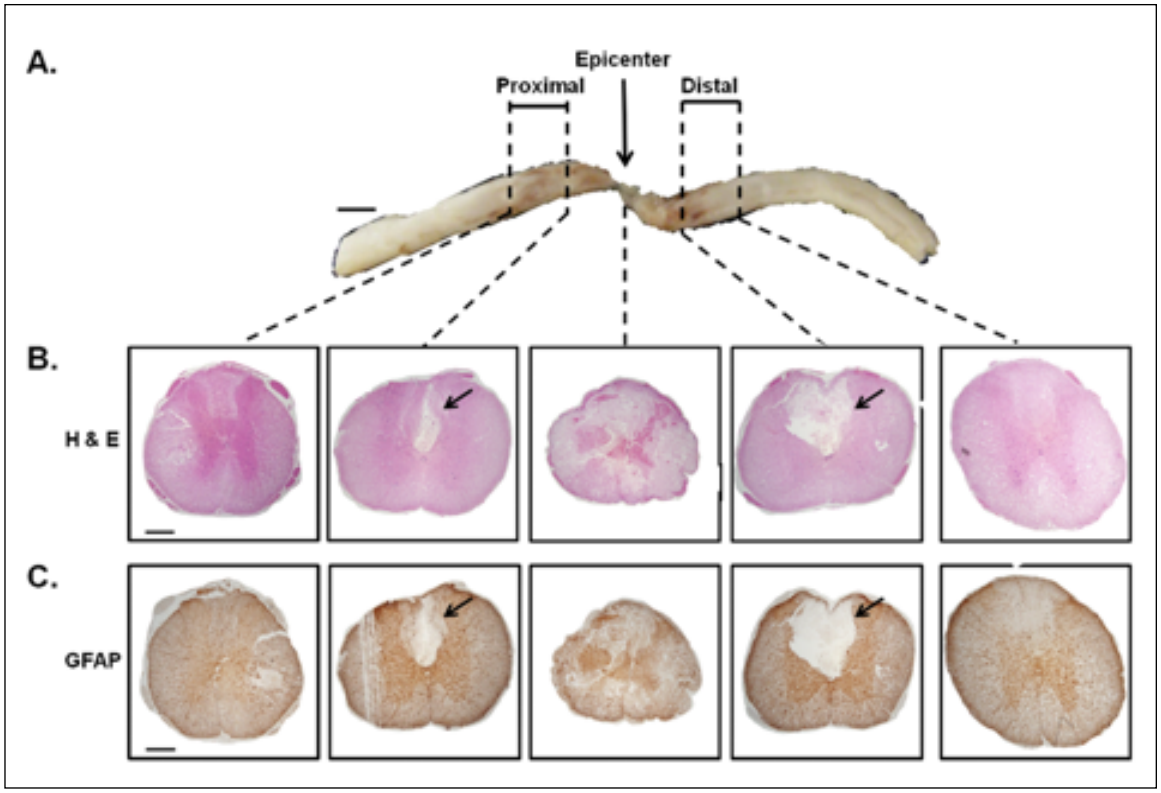

Figure 3.6 Representative gross anatomical representation of the spinal cords 24 hrs. after 7mm distraction injury. A) The epicenter of the injury shows a dramatic reduction in tissue volume that gradually improves 5mm from the lesion site. B) H & E histochemistry and C) visualization of GFAP-positive reactive astrocytes confirmed the extent of the lesion at, and near to the injury epicenter. Arrows indicate the areas of decellularity. Scale bar = 3mm (A) and 500 μm (B and C)

The extent of SCI produced by the 7 mm distraction was confirmed by the evident stretching of the spinal cord, which reduced the diameter of the cord at the epicenter of the lesion (Fig. 3.6 A). Histological evaluation revealed a highly localized injury, with a stretched epicenter exhibiting massive cell death extending both anterior and posterior from the epicenter, affecting the dorsal columns and sparing most of the ventral cord and white matter tracts in sections adjacent to the injury site (Fig 3.6 B). This characteristic lesion configuration was also confirmed by the immunostaining of reactive astrocytes, macrophages, and neuronal cell

bodies, which were localized at the lesion epicenter and circumvented the injured dorsal columns both proximally and distally to the distraction site (Fig. 3.6 C, Fig. 3.7 A,B). The upregulation of GFAP at the injury site is consistent with that traditionally observed in other models of spinal cord injury [101-102]. However, the specific ellipsoid shape of the acellular region due to cell death, and demarcation by the GFAP-positive reactive astrocytes, macrophages, and neuronal cell bodies seems unique to this injury paradigm.

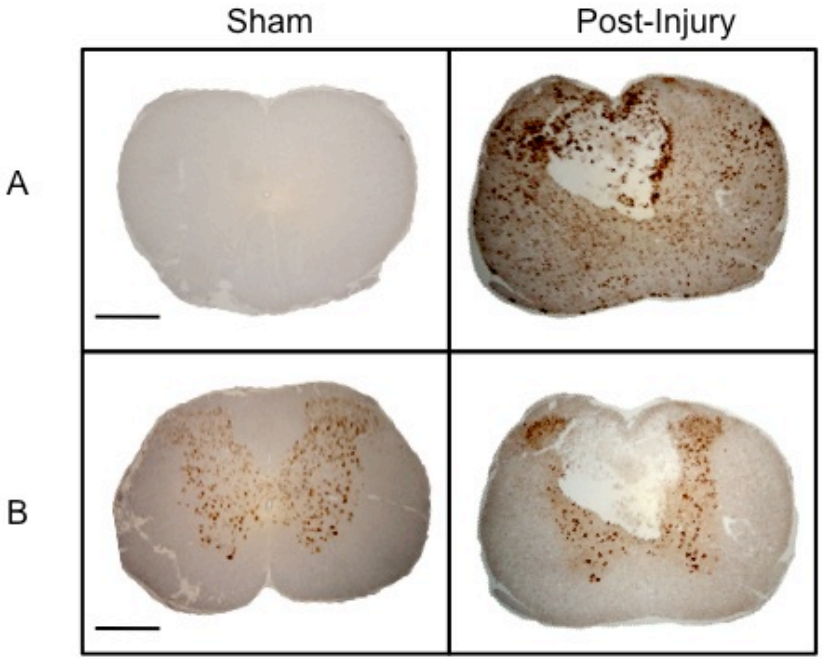

Figure 3.7 A) Spinal cord cross sections stained for ED1, post injury tissue shows massive amounts of macrophages. B) NueN stains show obliteration of neuronal cell bodies post injury. Scale bar = 500 μm

The massive cell death results from acute necrosis due to the excessive mechanical tissue distention. This is followed by secondary injury events that ultimately result in apoptotic cell death [103-105] including vascular leakage, ischemia-reperfusion, glutamate excitotoxicity and disturbances in ionic homeostasis, oxidative cell injury and inflammation [10, 106-107]. Overall, the histological evaluation indicated that the 7 mm bidirectional spine distraction caused

reproducibly severe and highly localized damage to the spinal cord, which explains the dramatic loss of function observed in all animals.

Table 3.1 Force Data

Animal Number	Initial Tension (N)	Peak Force (N)
Sham 1	3	-
Sham 2	3.8	-
Sham 3	3.9	-
Rat 1	5.2	23.4
Rat 2	3.4	25.9
Rat 3	4.6	18.8
Rat 4	4.2	26.1
Rat 5	4	26.5
Rat 6	3.7	31.6
Average	4.0	25.4
Standard Deviation	0.6	4.2

Force data was recorded during all distractions (Table 3.1). The average initial gentle tension applied to each animal was calculated to be 4.0 ± .6N. Figure 3.8 shows a representation of the time series data after initial tension was applied and load cell recalibrated back to 0 before distraction. The average peak force recorded during distraction was 25.4 ± 4.2N. Force data only allows us to characterize the force of distraction at the vertebral bodies, and does not represent forces actually occurring to the spinal cord itself.

During scoliosis surgery, the predominant correction technique is translation of tensile forces along the axis of the screws perpendicular to the intended rod direction that applies distraction and/or compression forces for the correction and fixation of the curve [108-110]. The histological and behavioral data strongly suggest that a 7 mm distraction in the rat is unnecessarily drastic for modeling the axial pullout of the spine during surgical correction in scoliosis. A distraction of 7 mm created a vertebral separation equivalent to 2 vertebral segments in the rat [111-112]. Since the human thoracic spine contains 12 vertebral segments and

averages 28 cm in length [113-115], if extrapolated, such separation approximates 46 mm in adult humans, a defect which will require forces normally not applied during scoliosis distraction and spine instrumentation and which is unlikely to occur during surgery. The severity of the 7 mm distraction in the rat better resembles shear fracture-dislocations of the thoracic and lumbar spine associated with forceful hyperextension (i.e., Lumberjack Paraplegia) [116-117].

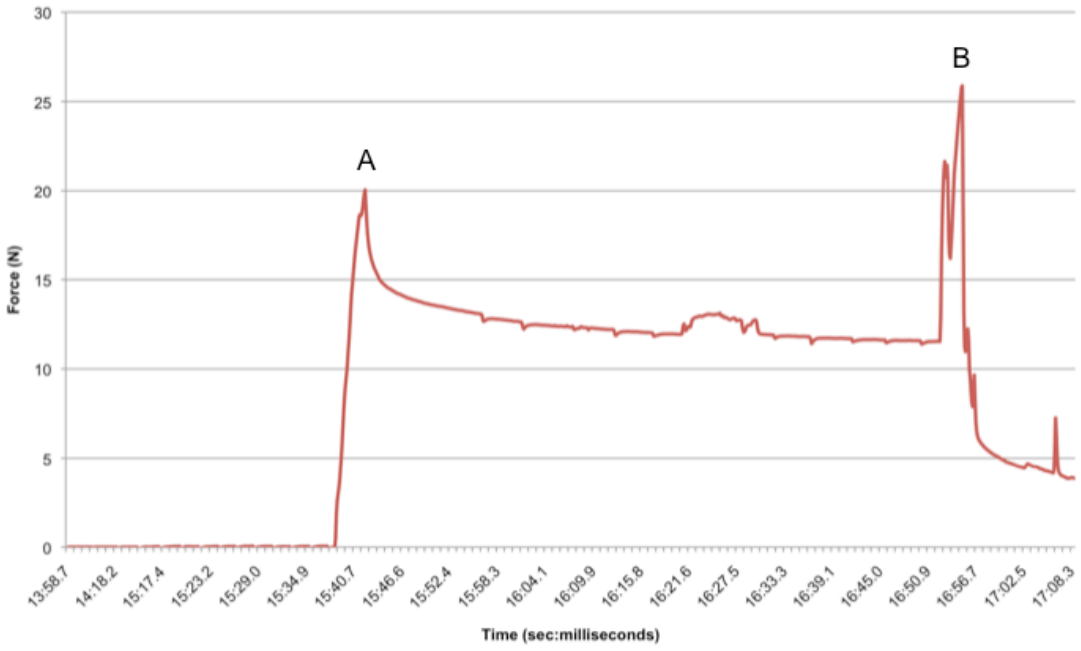

Figure 3.8 A representative force over time series during distraction. A) Shows an event that increased force possibly the breaking of attached muscle or tendon. B) Peak Force recorded during distraction.

3.2 Conclusion

The UTA distractor device here reported allows the application of highly controlled distraction to the rat spine. Therefore, we are currently evaluating the impact of various distraction paradigms on the degree of induced SCI, in order to determine a specific protocol that will better approximate the type of injury and forces typically created during scoliosis corrective surgery.

The development of a highly reproducible animal model of spine distraction and consequent SCI, will contribute significantly as a test platform on which several neuroprotective strategies can be screened for their ability to prevent unintended new neurological damage during spine surgery. Such research may allow for the development of neuroprotective therapies that can eventually minimize or eliminate the development of new neurological deficits in patients undergoing corrective spine surgery.

CHAPTER 4

FUTURE WORK

4.1 Limitations

We acknowledge the animal model described here for spine corrective surgeries has limitations. 1) TcMEPs were only taken before and immediately after distraction took place, and were not recorded during the actual distraction movement. Surgeons, in contrast, constantly monitor TcMEPs throughout the process of correction. 2) A deformity correction surgery can last 6-8 hours and distraction forces utilized for the entire duration of the surgery. This model of distraction lasted approximately 3.5seconds. 3) Scoliosis is a very convoluted spine deformity involving lateral deviation and rotation of vertebral bodies, and currently there are not animals that come with pre determined spine deformities, therefore our model does not represent injury caused to rotation or realignment from lateral deviation; this model only mimics the stretching/distraction force used to help in spine realignment. 4) Forces calculated represent only that which is happening to the vertebral bodies themselves and cannot be directly correlated to that which is taking place to the actual spinal cord.

4.2 Future Strategies

Protecting against physical destruction of spinal cord neurons after severe SCI is very difficult to do. The UTA distractor device was successful in reproducing controlled injuries, and now more work must be done to define and characterize less severe SCI. In order to address limitations stated above future work will involve the study of a graded SCI, which will involve characterization of behavior, histology, intraoperative monitoring, and other variables by distracting at different distances and/or speeds. This will allow us to more closely mimic the duration of scoliosis surgery and enable us to record TcMEPs during the distraction as a surgeon would. Also other studies can be done on the effects of small amounts of stretch held

for long periods of time. In this study, neurological deficits may not come from the primary mechanical destruction of tissue, but may point to specific secondary mechanisms that are in play.

As stated in the limitations, the current device can only simulate stretching forces used in spine deformity correction and does not allow us to simulate the lateral deviations associated with deformity. To improve the animal model, future work will also involve the automation of lateral moving platforms. Lateral moving platforms will allow for clamps not only to be moved in the y-axis, simulating stretching forces, but x-axis simultaneously, which will simulate the lateral forces surgeons use to align the spine.

In order to improve force measurements imparted directly to the spinal cord neurons, and not just the vertebral column, different tissue measuring strategies will be explored. This may involve tissue markers placed directly on the spinal cord, high speed digital photography to capture tissue movement, or the use of intraoperative radiograph and radiograph labels.

Overcoming these limitations will establish a more complete animal model for spine deformity correction in the future. Since there is currently no successful SCI treatment available, the ultimate goal of future work using the UTA distractor device is to screen for neurological treatments that would be used to reduce, eliminate, and protect patients from deficits that may be caused during deformity surgery and other SCIs.

REFERENCES

1. Luchetti S, Beck KD, Galvan MD, Silva R, Cummings BJ, Anderson AJ. Comparison of immunopathology and locomotor recovery in C57BL/6, BUB/BnJ, and NOD-SCID mice after contusion spinal cord injury. *J Neurotrauma*. 2010;27(2):411-421. 10.1089/neu.2009.0930.
2. McDonald JW, Sadowsky C. Spinal-cord injury. *The Lancet*. 2002;359(9304):417-425. DOI: 10.1016/S0140-6736(02)07603-1.
3. Jackson AB, Dijkers M, Devivo MJ, Poczatek RB. A demographic profile of new traumatic spinal cord injuries: change and stability over 30 years. *Arch Phys Med Rehabil*. 2004;85(11):1740-1748.
4. Choo AM, Liu J, Lam CK, Dvorak M, Tetzlaff W, Oxland TR. Contusion, dislocation, and distraction: primary hemorrhage and membrane permeability in distinct mechanisms of spinal cord injury. *J Neurosurg Spine*. 2007;6(3):255-266. 10.3171/spi.2007.6.3.255.
5. Pickett GE, Campos-Benitez M, Keller JL, Duggal N. Epidemiology of traumatic spinal cord injury in Canada. *Spine (Phila Pa 1976)*. 2006;31(7):799-805. 10.1097/01.brs.0000207258.80129.03.
6. The National SCI Database. US National Spinal Cord Injury. Available at: http://www.spinalcord.uab.edu
7. Wyndaele M, Wyndaele JJ. Incidence, prevalence and epidemiology of spinal cord injury: what learns a worldwide literature survey? *Spinal Cord*. 2006;44(9):523-529. 10.1038/sj.sc.3101893.
8. McColl MA, Walker J, Stirling P, Wilkins R, Corey P. Expectations of life and health among spinal cord injured adults. *Spinal Cord*. 1997;35(12):818-828.

9. Sadowsky CL, Margherita A. The Cost of Spinal Cord Injury Care. *Spine: State of the Art Reviews*. 1999;13(3):593-606.

10. Sekhon LH, Fehlings MG. Epidemiology, demographics, and pathophysiology of acute spinal cord injury. *Spine (Phila Pa 1976)*. 2001;26(24 Suppl):S2-12.

11. Magerl F, Aebi M, Gertzbein SD, Harms J, Nazarian S. A comprehensive classification of thoracic and lumbar injuries. *Eur Spine J*. 1994;3(4):184-201.

12. Fehlings MG, Tator CH. An evidence-based review of decompressive surgery in acute spinal cord injury: rationale, indications, and timing based on experimental and clinical studies. *J Neurosurg*. 1999;91(1 Suppl):1-11.

13. Brösamle C, Huber AB. Cracking the black box – and putting it back together again: Animal models of spinal cord injury. *Drug Discovery Today: Disease Models*. 2006;3(4):341-347. DOI: 10.1016/j.ddmod.2006.11.006.

14. Courtine G, Bunge MB, Fawcett JW, et al. Can experiments in nonhuman primates expedite the translation of treatments for spinal cord injury in humans? *Nat Med*. 2007;13(5):561-566. 10.1038/nm1595.

15. Fernandez E, Pallini R, Lauretti L, Mercanti D, Serra A, Calissano P. Spinal cord transection in adult rats: effects of local infusion of nerve growth factor on the corticospinal tract axons. *Neurosurgery*. 1993;33(5):889-893.

16. Bregman BS, Coumans JV, Dai HN, et al. Transplants and neurotrophic factors increase regeneration and recovery of function after spinal cord injury. *Prog Brain Res*. 2002;137:257-273.

17. Ramon-Cueto A, Cordero MI, Santos-Benito FF, Avila J. Functional recovery of paraplegic rats and motor axon regeneration in their spinal cords by olfactory ensheathing glia. *Neuron*. 2000;25(2):425-435.

18. Fouad K, Schnell L, Bunge MB, Schwab ME, Liebscher T, Pearse DD. Combining Schwann cell bridges and olfactory-ensheathing glia grafts with chondroitinase

promotes locomotor recovery after complete transection of the spinal cord. *J Neurosci*. 2005;25(5):1169-1178. 10.1523/JNEUROSCI.3562-04.2005.

19. Bareyre FM, Kerschensteiner M, Raineteau O, Mettenleiter TC, Weinmann O, Schwab ME. The injured spinal cord spontaneously forms a new intraspinal circuit in adult rats. *Nat Neurosci*. 2004;7(3):269-277. 10.1038/nn1195.
20. Coumans JV, Lin TT, Dai HN, et al. Axonal regeneration and functional recovery after complete spinal cord transection in rats by delayed treatment with transplants and neurotrophins. *J Neurosci*. 2001;21(23):9334-9344.
21. Basso DM, Beattie MS, Bresnahan JC. Graded histological and locomotor outcomes after spinal cord contusion using the NYU weight-drop device versus transection. *Exp Neurol*. 1996;139(2):244-256. 10.1006/exnr.1996.0098.
22. Moon L, Bunge MB. From animal models to humans: strategies for promoting CNS axon regeneration and recovery of limb function after spinal cord injury. *J Neurol Phys Ther*. 2005;29(2):55-69.
23. Tator CH. Review of experimental spinal cord injury with emphasis on the local and systemic circulatory effects. *Neurochirurgie*. 1991;37(5):291-302.
24. HOWLAND WJ, CURRY JL, BUFFINGTON CB. Fulcrum Fractures of the Lumbar Spine. Transverse Fracture Induced by an Improperly Placed Seat Belt. *JAMA*. 1965;193:240-241.
25. Koyanagi I, Tator CH, Theriault E. Silicone rubber microangiography of acute spinal cord injury in the rat. *Neurosurgery*. 1993;32(2):260-8; discussion 268.
26. Kwon BK, Tetzlaff W, Grauer JN, Beiner J, Vaccaro AR. Pathophysiology and pharmacologic treatment of acute spinal cord injury. *Spine J*. 2004;4(4):451-464. 10.1016/j.spinee.2003.07.007.
27. Tator CH, Koyanagi I. Vascular mechanisms in the pathophysiology of human spinal cord injury. *J Neurosurg*. 1997;86(3):483-492. 10.3171/jns.1997.86.3.0483.

28. Lukacova N, Halat G, Chavko M, Marsala J. Ischemia-reperfusion injury in the spinal cord of rabbits strongly enhances lipid peroxidation and modifies phospholipid profiles. *Neurochem Res*. 1996;21(8):869-873.

29. Basu S, Hellberg A, Ulus AT, Westman J, Karacagil S. Biomarkers of free radical injury during spinal cord ischemia. *FEBS Lett*. 2001;508(1):36-38.

30. Genovese T, Cuzzocrea S. Role of free radicals and poly(ADP-ribose)polymerase-1 in the development of spinal cord injury: new potential therapeutic targets. *Curr Med* Chem. 2008;15(5):477-487.

31. Xiong Y, Rabchevsky AG, Hall ED. Role of peroxynitrite in secondary oxidative damage after spinal cord injury. *J Neurochem*. 2007;100(3):639-649. 10.1111/j.1471-4159.2006.04312.x.

32. McDonald JW, Althomsons SP, Hyrc KL, Choi DW, Goldberg MP. Oligodendrocytes from forebrain are highly vulnerable to AMPA/kainate receptor-mediated excitotoxicity. *Nat Med*. 1998;4(3):291-297.

33. Li S, Stys PK. Mechanisms of ionotropic glutamate receptor-mediated excitotoxicity in isolated spinal cord white matter. *J Neurosci*. 2000;20(3):1190-1198.

34. Pitt D, Nagelmeier IE, Wilson HC, Raine CS. Glutamate uptake by oligodendrocytes: Implications for excitotoxicity in multiple sclerosis. *Neurology*. 2003;61(8):1113-1120.

35. Schwartz M, Moalem G, Leibowitz-Amit R, Cohen IR. Innate and adaptive immune responses can be beneficial for CNS repair. *Trends Neurosci*. 1999;22(7):295-299.

36. Popovich PG, Wei P, Stokes BT. Cellular inflammatory response after spinal cord injury in Sprague-Dawley and Lewis rats. *J Comp Neurol*. 1997;377(3):443-464.

37. Massey JM, Amps J, Viapiano MS, et al. Increased chondroitin sulfate proteoglycan expression in denervated brainstem targets following spinal cord injury creates a barrier to axonal regeneration overcome by chondroitinase ABC and neurotrophin-3. *Exp Neurol*. 2008;209(2):426-445. 10.1016/j.expneurol.2007.03.029.

38. Donnelly DJ, Popovich PG. Inflammation and its role in neuroprotection, axonal regeneration and functional recovery after spinal cord injury. *Exp Neurol*. 2008;209(2):378-388. 10.1016/j.expneurol.2007.06.009.

39. Emery E, Aldana P, Bunge MB, et al. Apoptosis after traumatic human spinal cord injury. J *Neurosurg*. 1998;89(6):911-920. 10.3171/jns.1998.89.6.0911.

40. Crowe MJ, Bresnahan JC, Shuman SL, Masters JN, Beattie MS. Apoptosis and delayed degeneration after spinal cord injury in rats and monkeys. *Nat Med*. 1997;3(1):73-76.

41. Casha S, Yu WR, Fehlings MG. Oligodendroglial apoptosis occurs along degenerating axons and is associated with FAS and p75 expression following spinal cord injury in the rat. *Neuroscience*. 2001;103(1):203-218.

42. Diaz-Ruiz A, Rios C, Duarte I, et al. Cyclosporin-A inhibits lipid peroxidation after spinal cord injury in rats. *Neurosci Lett*. 1999;266(1):61-64.

43. Guha A, Tator CH, Rochon J. Spinal cord blood flow and systemic blood pressure after experimental spinal cord injury in rats. *Stroke*. 1989;20(3):372-377.

44. Tator CH. Hemodynamic issues and vascular factors in acute experimental spinal cord injury. *J Neurotrauma*. 1992;9(2):139-40; discussion 141.

45. Stirling DP, Khodarahmi K, Liu J, et al. Minocycline treatment reduces delayed oligodendrocyte death, attenuates axonal dieback, and improves functional outcome after spinal cord injury. *J Neurosci*. 2004;24(9):2182-2190. 10.1523/JNEUROSCI.5275-03.2004.

46. Gris D, Marsh DR, Oatway MA, et al. Transient blockade of the CD11d/CD18 integrin reduces secondary damage after spinal cord injury, improving sensory, autonomic, and motor function. *J Neurosci*. 2004;24(16):4043-4051. 10.1523/JNEUROSCI.5343-03.2004.

47. Xu J, Fan G, Chen S, Wu Y, Xu XM, Hsu CY. Methylprednisolone inhibition of TNF-alpha expression and NF-kB activation after spinal cord injury in rats. *Brain Res Mol Brain Res*. 1998;59(2):135-142.

48. Wrathall JR, Teng YD, Choiniere D. Amelioration of functional deficits from spinal cord trauma with systemically administered NBQX, an antagonist of non-N-methyl-D-aspartate receptors. *Exp Neurol*. 1996;137(1):119-126. 10.1006/exnr.1996.0012.

49. Faden AI, Lemke M, Simon RP, Noble LJ. N-methyl-D-aspartate antagonist MK801 improves outcome following traumatic spinal cord injury in rats: behavioral, anatomic, and neurochemical studies. *J Neurotrauma*. 1988;5(1):33-45.

50. Gaviria M, Privat A, d'Arbigny P, Kamenka JM, Haton H, Ohanna F. Neuroprotective effects of gacyclidine after experimental photochemical spinal cord lesion in adult rats: dose-window and time-window effects. J *Neurotrauma*. 2000;17(1):19-30.

51. Bracken MB, Shepard MJ, Collins WF, et al. A randomized, controlled trial of methylprednisolone or naloxone in the treatment of acute spinal-cord injury. Results of the Second National Acute Spinal Cord Injury Study. *N Engl J Med*. 1990;322(20):1405-1411. 10.1056/NEJM199005173222001.

52. Bracken MB, Shepard MJ, Holford TR, et al. Administration of methylprednisolone for 24 or 48 hours or tirilazad mesylate for 48 hours in the treatment of acute spinal cord injury. Results of the Third National Acute Spinal Cord Injury Randomized Controlled Trial. National Acute Spinal Cord Injury Study. *JAMA*. 1997;277(20):1597-1604.

53. Hurlbert RJ, Hamilton MG. Methylprednisolone for acute spinal cord injury: 5-year practice reversal. *Can J Neurol Sci*. 2008;35(1):41-45.

54. Lee JM, Yan P, Xiao Q, et al. Methylprednisolone protects oligodendrocytes but not neurons after spinal cord injury. *J Neurosci*. 2008;28(12):3141-3149. 10.1523/JNEUROSCI.5547-07.2008.

55. Miller SM. Methylprednisolone in acute spinal cord injury: a tarnished standard. *J Neurosurg Anesthesiol*. 2008;20(2):140-142. 10.1097/01.ana.0000314442.40952.0d.

56. Vitale MG, Moore DW, Matsumoto H, et al. Risk factors for spinal cord injury during surgery for spinal deformity. *J Bone Joint Surg Am*. 2010;92(1):64-71. 10.2106/JBJS.H.01839.

57. Weinstein SL, Dolan LA, Cheng JC, Danielsson A, Morcuende JA. Adolescent idiopathic scoliosis. *Lancet*. 2008;371(9623):1527-1537. 10.1016/S0140-6736(08)60658-3.

58. Riseborough EJ, Wynne-Davies R. A genetic survey of idiopathic scoliosis in Boston, Massachusetts. *J Bone Joint Surg Am*. 1973;55(5):974-982.

59. Miller NH. Genetics of familial idiopathic scoliosis. *Clin Orthop Relat Res*. 2007;462:6-10. 10.1097/BLO.0b013e318126c062.

60. Lowe TG, Edgar M, Margulies JY, et al. Etiology of idiopathic scoliosis: current trends in research. *J Bone Joint Surg Am*. 2000;82-A(8):1157-1168.

61. Burwell RG. Aetiology of idiopathic scoliosis: current concepts. *Pediatr Rehabil*. 2003;6(3-4):137-170. 10.1080/13638490310001642757.

62. Young W. Chapter 17 Spinal cord contusion models. In: L. McKerracher GDaSR, ed. Progress in Brain Research. Vol Volume 137. Elsevier; 2002:231-255. DOI: 10.1016/S0079-6123(02)37019-5.

63. Carter OD, Haynes SG. Prevalence rates for scoliosis in US adults: results from the first National Health and Nutrition Examination Survey. *Int J Epidemiol*. 1987;16(4):537-544.

64. Schwab F, el-Fegoun AB, Gamez L, Goodman H, Farcy JP. A lumbar classification of scoliosis in the adult patient: preliminary approach. *Spine (Phila Pa 1976)*. 2005;30(14):1670-1673.

65. Perennou D, Marcelli C, Herisson C, Simon L. Adult lumbar scoliosis. Epidemiologic aspects in a low-back pain population. *Spine (Phila Pa 1976)*. 1994;19(2):123-128.

66. Francis RS. Scoliosis screening of 3,000 college-aged women. The Utah Study--phase 2. *Phys Ther*. 1988;68(10):1513-1516.

67. Carman DL, Browne RH, Birch JG. Measurement of scoliosis and kyphosis radiographs. Intraobserver and interobserver variation. *J Bone Joint Surg Am*. 1990;72(3):328-333.

68. Morrissy RT, Goldsmith GS, Hall EC, Kehl D, Cowie GH. Measurement of the Cobb on radiographs of patients who have scoliosis. Evaluation of intrinsic error. *J Bone Joint Surg Am*. 1990;72(3):320-327.

69. Fallstrom K, Cochran T, Nachemson A. Long-term effects on personality development in patients with adolescent idiopathic scoliosis. Influence of type of treatment. *Spine (Phila Pa 1976)*. 1986;11(7):756-758.

70. Tones M, Moss N, Polly DW,Jr. A review of quality of life and psychosocial issues in scoliosis. *Spine (Phila Pa 1976)*. 2006;31(26):3027-3038. 10.1097/01.brs.0000249555.87601.fc.

71. Matsunaga S, Hayashi K, Naruo T, Nozoe S, Komiya S. Psychologic management of brace therapy for patients with idiopathic scoliosis. *Spine (Phila Pa 1976)*. 2005;30(5):547-550.

72. Buchowski JM, Bhatnagar R, Skaggs DL, Sponseller PD. Temporary internal distraction as an aid to correction of severe scoliosis. *J Bone Joint Surg Am*. 2006;88(9):2035-2041. 10.2106/JBJS.E.00823.

73. Buchowski JM, Skaggs DL, Sponseller PD. Temporary internal distraction as an aid to correction of severe scoliosis. Surgical technique. *J Bone Joint Surg Am*. 2007;89 Suppl 2 Pt.2:297-309. 10.2106/JBJS.G.00163.

74. Mooney JF,3rd, Bernstein R, Hennrikus WL,Jr, MacEwen GD. Neurologic risk management in scoliosis surgery. *J Pediatr Orthop*. 2002;22(5):683-689.

75. Orchowski J, Bridwell KH, Lenke LG. Neurological deficit from a purely vascular etiology after unilateral vessel ligation during anterior thoracolumbar fusion of the spine. *Spine (Phila Pa 1976)*. 2005;30(4):406-410.

76. Schulte TL, Lerner T, Berendes E, et al. Transient hemiplegia in posterior instrumentation of scoliosis. *Spine (Phila Pa 1976)*. 2004;29(18):E394-8.

77. Qiu Y, Wang S, Wang B, Yu Y, Zhu F, Zhu Z. Incidence and risk factors of neurological deficits of surgical correction for scoliosis: analysis of 1373 cases at one Chinese institution. *Spine (Phila Pa 1976)*. 2008;33(5):519-526. 10.1097/BRS.0b013e3181657d93.

78. Winter RB. Neurologic safety in spinal deformity surgery. *Spine (Phila Pa 1976)*. 1997;22(13):1527-1533.

79. MacEwen GD, Bunnell WP, Sriram K. Acute neurological complications in the treatment of scoliosis. A report of the Scoliosis Research Society. *J Bone Joint Surg Am*. 1975;57(3):404-408.

80. Dutoit M, Rigault P, Pouliquen JC, et al. Surgical treatment of scoliosis of 100 degrees and greater in children and adolescents (neurological and myopathic scoliosis excluded). Apropos of a series of 66 cases. *Rev Chir Orthop Reparatrice Appar Mot*. 1985;71(8):549-562.

81. Thuet ED, Winscher JC, Padberg AM, et al. Validity and reliability of intraoperative monitoring in pediatric spinal deformity surgery: a 23-year experience of 3436 surgical cases. *Spine (Phila Pa 1976)*. 2010;35(20):1880-1886. 10.1097/BRS.0b013e3181e53434.

82. Owen JH. The application of intraoperative monitoring during surgery for spinal deformity. *Spine (Phila Pa 1976)*. 1999;24(24):2649-2662.

83. Nuwer MR, Dawson EG, Carlson LG, Kanim LE, Sherman JE. Somatosensory evoked potential spinal cord monitoring reduces neurologic deficits after scoliosis surgery:

results of a large multicenter survey. *Electroencephalogr Clin Neurophysiol*. 1995;96(1):6-11.

84. Kamerlink JR, Errico T, Xavier S, et al. Major intraoperative neurologic monitoring deficits in consecutive pediatric and adult spinal deformity patients at one institution. *Spine (Phila Pa 1976)*. 2010;35(2):240-245. 10.1097/BRS.0b013e3181c7c8f6.

85. Accadbled F, Henry P, de Gauzy JS, Cahuzac JP. Spinal cord monitoring in scoliosis surgery using an epidural electrode. Results of a prospective, consecutive series of 191 cases. *Spine (Phila Pa 1976).* 2006;31(22):2614-2623. 10.1097/01.brs.0000240642.28495.99.

86. Alfred RA, Surgery of experimental lesion of spinal cord equivalent to crush injury of fracture dislocation of spinal column. *JAMA*. 1911;LVII(11):878-880.

87. Anderson TE, Stokes BT. Experimental models for spinal cord injury research: physical and physiological considerations. *J Neurotrauma*. 1992;9 Suppl 1:S135-42.

88. Gruner JA. A monitored contusion model of spinal cord injury in the rat. *J Neurotrauma*. 1992;9(2):123-6; discussion 126-8.

89. Jakeman LB, Guan Z, Wei P, et al. Traumatic spinal cord injury produced by controlled contusion in mouse. *J Neurotrauma*. 2000;17(4):299-319.

90. Noyes DH. Electromechanical impactor for producing experimental spinal cord injury in animals. *Med Biol Eng Comput*. 1987;25(3):335-340.

91. Young W. Spinal cord contusion models. *Prog Brain Res*. 2002;137:231-255.

92. Kwon BK, Oxland TR, Tetzlaff W. Animal models used in spinal cord regeneration research. *Spine (Phila Pa 1976)*. 2002;27(14):1504-1510.

93. Rabchevsky AG, Fugaccia I, Sullivan PG, Blades DA, Scheff SW. Efficacy of methylprednisolone therapy for the injured rat spinal cord. *J Neurosci Res*. 2002;68(1):7-18.

94. Fiford RJ, Bilston LE, Waite P, Lu J. A vertebral dislocation model of spinal cord injury in rats. *J Neurotrauma*. 2004;21(4):451-458. 10.1089/089771504323004593.

95. Dabney KW, Ehrenshteyn M, Agresta CA, et al. A model of experimental spinal cord trauma based on computer-controlled intervertebral distraction: characterization of graded injury. *Spine (Phila Pa 1976)*. 2004;29(21):2357-2364.

96. Choo AM, Liu J, Liu Z, Dvorak M, Tetzlaff W, Oxland TR. Modeling spinal cord contusion, dislocation, and distraction: characterization of vertebral clamps, injury severities, and node of Ranvier deformations. *J Neurosci Methods*. 2009;181(1):6-17. 10.1016/j.jneumeth.2009.04.007.

97. TARLOV IM, KLINGER H. Spinal cord compression studies. II. Time limits for recovery after acute compression in dogs. *AMA Arch Neurol Psychiatry*. 1954;71(3):271-290.

98. Basso DM, Beattie MS, Bresnahan JC. A sensitive and reliable locomotor rating scale for open field testing in rats. J *Neurotrauma*. 1995;12(1):1-21.

99. Basso DM, Beattie MS, Bresnahan JC, et al. MASCIS evaluation of open field locomotor scores: effects of experience and teamwork on reliability. Multicenter Animal Spinal Cord Injury Study. J *Neurotrauma*. 1996;13(7):343-359.

100. Choo AM, Liu J, Dvorak M, Tetzlaff W, Oxland TR. Secondary pathology following contusion, dislocation, and distraction spinal cord injuries. *Exp Neurol*. 2008;212(2):490-506. 10.1016/j.expneurol.2008.04.038.

101. Herrmann JE, Shah RR, Chan AF, Zheng B. EphA4 deficient mice maintain astroglial-fibrotic scar formation after spinal cord injury. *Exp Neurol*. 2010;223(2):582-598. 10.1016/j.expneurol.2010.02.005.

102. Sofroniew MV. Molecular dissection of reactive astrogliosis and glial scar formation. *Trends Neurosci*. 2009;32(12):638-647. 10.1016/j.tins.2009.08.002.

103. Galluzzi L, Maiuri MC, Vitale I, et al. Cell death modalities: classification and pathophysiological implications. *Cell Death Differ*. 2007;14(7):1237-1243. 10.1038/sj.cdd.4402148.

104. Kawabata H, Setoguchi T, Yone K, et al. High mobility group box 1 is upregulated after spinal cord injury and is associated with neuronal cell apoptosis. *Spine (Phila Pa 1976)*. 2010;35(11):1109-1115. 10.1097/BRS.0b013e3181bd14b6.

105. Liu XZ, Xu XM, Hu R, et al. Neuronal and glial apoptosis after traumatic spinal cord injury. *J Neurosci*. 1997;17(14):5395-5406.

106. Campos-Esparza MR, Sanchez-Gomez MV, Matute C. Molecular mechanisms of neuroprotection by two natural antioxidant polyphenols. *Cell Calcium*. 2009;45(4):358-368. 10.1016/j.ceca.2008.12.007.

107. Yong C, Arnold PM, Zoubine MN, et al. Apoptosis in cellular compartments of rat spinal cord after severe contusion injury. *J Neurotrauma*. 1998;15(7):459-472.

108. Lee SM, Suk SI, Chung ER. Direct vertebral rotation: a new technique of three-dimensional deformity correction with segmental pedicle screw fixation in adolescent idiopathic scoliosis. *Spine (Phila Pa 1976)*. 2004;29(3):343-349.

109. Liljenqvist U, Hackenberg L, Link T, Halm H. Pullout strength of pedicle screws versus pedicle and laminar hooks in the thoracic spine. *Acta Orthop Belg*. 2001;67(2):157-163.

110. Wenger DR, Carollo JJ, Wilkerson JA,Jr. Biomechanics of scoliosis correction by segmental spinal instrumentation. *Spine (Phila Pa 1976)*. 1982;7(3):260-264.

111. Flynn JR, Bolton PS. Measurement of the vertebral canal dimensions of the neck of the rat with a comparison to the human. *Anat Rec (Hoboken)*. 2007;290(7):893-899. 10.1002/ar.20523.

112. Porter RW. Idiopathic scoliosis: the relation between the vertebral canal and the vertebral bodies. *Spine (Phila Pa 1976)*. 2000;25(11):1360-1366.

113. Liljenqvist UR, Allkemper T, Hackenberg L, Link TM, Steinbeck J, Halm HF. Analysis of vertebral morphology in idiopathic scoliosis with use of magnetic resonance imaging and multiplanar reconstruction. *J Bone Joint Surg Am*. 2002;84-A(3):359-368.

114. Panjabi MM, Takata K, Goel V, et al. Thoracic human vertebrae. Quantitative three-dimensional anatomy. *Spine (Phila Pa 1976)*. 1991;16(8):888-901.

115. Sucato DJ, Duchene C. The position of the aorta relative to the spine: a comparison of patients with and without idiopathic scoliosis. *J Bone Joint Surg Am*. 2003;85-A(8):1461-1469.

116. Denis F, Burkus JK. Shear fracture-dislocations of the thoracic and lumbar spine associated with forceful hyperextension (lumberjack paraplegia). *Spine (Phila Pa 1976)*. 1992;17(2):156-161.

117. Erb R, Glassman S, Edwards J, Nance E. Hyperextension fracture-dislocation of the thoracic spine. *Emergency Radiology*. 1995;2(4):237-240.

BIOGRAPHICAL INFORMATION

Bradley B Elmer was born on 22 June 1983. He served a 2-year mission in Leon, Mexico for the Church of Jesus Christ of Latter-Day Saints from 2002-2004. While pursuing his undergraduate studies he worked as a 911 dispatcher and volunteer EMT, where he developed a great interest in the healthcare field. In May 2008, he received his Bachelor's degree in Mechanical Engineering from Brigham Young University. To further his knowledge in the field emergency services he attended and graduated from the Recruit Candidate Academy at Utah's Fire and Rescue Academy in December 2008. Wanting to pursue a career in medical device product development he joined the University of Texas at Arlington/University of Texas Southwestern Medical Center joint Biomedical Engineering program in January 2009, and subsequently Dr. Mario Romero-Ortega's neural-regeneration lab. His ultimate goal is develop better technologies and devices that can be implemented to improve the quality of care in the emergency services field and safety of those responding.